NBS TECHNICAL NOTE 1008

U.S. DEPARTMENT OF COMMERCE/National Bureau of Standards

ANTENNAS AND THE ASSOCIATED TIME DOMAIN RANGE FOR THE MEASUREMENT OF IMPULSIVE FIELDS

NATIONAL BUREAU OF STANDARDS

The National Bureau of Standards[1] was established by an act of Congress March 3, 1901. The Bureau's overall goal is to strengthen and advance the Nation's science and technology and facilitate their effective application for public benefit. To this end, the Bureau conducts research and provides: (1) a basis for the Nation's physical measurement system, (2) scientific and technological services for industry and government, (3) a technical basis for equity in trade, and (4) technical services to promote public safety. The Bureau's technical work is performed by the National Measurement Laboratory, the National Engineering Laboratory, and the Institute for Computer Sciences and Technology.

THE NATIONAL MEASUREMENT LABORATORY provides the national system of physical and chemical and materials measurement; coordinates the system with measurement systems of other nations and furnishes essential services leading to accurate and uniform physical and chemical measurement throughout the Nation's scientific community, industry, and commerce; conducts materials research leading to improved methods of measurement, standards, and data on the properties of materials needed by industry, commerce, educational institutions, and Government; provides advisory and research services to other Government Agencies; develops, produces, and distributes Standard Reference Materials; and provides calibration services. The Laboratory consists of the following centers:

Absolute Physical Quantities[2] — Radiation Research — Thermodynamics and Molecular Science — Analytical Chemistry — Materials Science.

THE NATIONAL ENGINEERING LABORATORY provides technology and technical services to users in the public and private sectors to address national needs and to solve national problems in the public interest; conducts research in engineering and applied science in support of objectives in these efforts; builds and maintains competence in the necessary disciplines required to carry out this research and technical service; develops engineering data and measurement capabilities; provides engineering measurement traceability services; develops test methods and proposes engineering standards and code changes; develops and proposes new engineering practices; and develops and improves mechanisms to transfer results of its research to the utlimate user. The Laboratory consists of the following centers:

Applied Mathematics — Electronics and Electrical Engineering[2] — Mechanical Engineering and Process Technology[2] — Building Technology — Fire Research — Consumer Product Technology — Field Methods.

THE INSTITUTE FOR COMPUTER SCIENCES AND TECHNOLOGY conducts research and provides scientific and technical services to aid Federal Agencies in the selection, acquisition, application, and use of computer technology to improve effectiveness and economy in Government operations in accordance with Public Law 89-306 (40 U.S.C. 759), relevant Executive Orders, and other directives; carries out this mission by managing the Federal Information Processing Standards Program, developing Federal ADP standards guidelines, and managing Federal participation in ADP voluntary standardization activities; provides scientific and technological advisory services and assistance to Federal Agencies; and provides the technical foundation for computer-related policies of the Federal Government. The Institute consists of the following divisions:

Systems and Software — Computer Systems Engineering — Information Technology.

[1]Headquarters and Laboratories at Gaithersburg, Maryland, unless otherwise noted; mailing address Washington,D.C. 20234.
[2]Some divisions within the center are located at Boulder, Colorado, 80303.

The National Bureau of Standards was reorganized, effective April 9, 1978.

ANTENNAS AND THE ASSOCIATED TIME DOMAIN RANGE FOR THE MEASUREMENT OF IMPULSIVE FIELDS

Robert A. Lawton

Arthur R. Ondrejka

Electromagnetic Technology Division
National Engineering Laboratory
National Bureau of Standards
Boulder, Colorado 80303

U.S. DEPARTMENT OF COMMERCE, Juanita M. Kreps, Secretary
Sidney Harman, Under Secretary
Jordan J. Baruch, Assistant Secretary for Science and Technology

NATIONAL BUREAU OF STANDARDS, Ernest Ambler, Director

Issued November 1978

NATIONAL BUREAU OF STANDARDS TECHNICAL NOTE 1008

Nat. Bur. Stand. (U.S.), Tech. Note 1008, 68 pages (Nov. 1978)

CODEN: NBTNAE

U.S. GOVERNMENT PRINTING OFFICE
WASHINGTON: 1978

For sale by the Superintendent of Documents, U.S. Government Printing Office, Washington, D.C. 20402

Stock No. 003-003-01998-4 Price $2.40 (Add 25 percent additional for other than U.S. mailing)

CONTENTS

ANTENNAS AND THE ASSOCIATED TIME DOMAIN RANGE FOR THE MEASUREMENT OF IMPULSIVE FIELDS

Robert A. Lawton and Arthur R. Ondrejka
Electromagnetic Technology Division
Center for Electronics and Electrical Engineering
National Bureau of Standards
Boulder, Colorado, 80303 U.S.A.

This report describes the construction and evaluation of a TEM horn antenna designed at NBS to be used as a transfer standard to generate and measure impulsive electromagnetic fields. Our purpose in the evaluation was to analyze the different electrical field generation and measurement techniques thoroughly enough to determine the major sources of error and establish a standard of impulsive field strength having a well established statement of accuracy.

The evaluation of this horn was done in two independent ways; by placing the horn in the field of a conical transmission line and by a three antenna intercomparison. The two methods were found to agree within ± 3 dB over the range of 0.6 to 5 GHz. Part of this disagreement is due to the assumption of far field conditions, and an experimental technique is described which determines the frequency range over which this assumption is valid.

Key words: Antenna; conical transmission line; impulsive fields; impulse response; standards; TEM horn antenna.

1. INTRODUCTION

Radar and its many applications for the military have been with us for some time now while civilian applications (other than speed traps), such as automobile collision avoidance and air bag inflation, have awaited the higher resolution that present state-of-the-art radars are just now making available. This development, together with digital communication systems which are now approaching the gigabit data rate, requires wideband antennas in order to achieve the required transient response.

Present techniques for evaluating the pertinent antenna parameters include:

1. Stepping or sweeping a cw generator and observing the response through identical transmitting and receiving antennas with a swept (or stepped) cw receiver such as an RFI meter, a spectrum analyzer, or an automatic network analyzer.
2. Feeding an rf burst through the antenna system and observing the response with either a spectrum analyzer, an RFI meter, or a sampling oscilloscope.
3. Feeding the antenna system with a baseband step or impulse from any one of a variety of generators, such as a tunnel diode, a step recovery diode, a spark gap, or a mercury switch, and observing the response with a sampling oscilloscope.
4. Feeding broadband noise through the antenna system and observing the response with a tuned receiver. Emission from radio stars has also been used as a standard for calibrating large radio telescopes.

The above procedures will result in a measure of the antenna transmission or transfer function, $H(s)$, or the impulse response, $h(t)$. The reflection coefficient, $\Gamma(s)$, and the analogous time domain parameter, $\gamma(t)$, the inverse Laplace transform of $\Gamma(s)$, can also be obtained. In terms of frequency domain scattering parameters, the transmission function is given by S_{21} and the reflection coefficient by S_{11}.

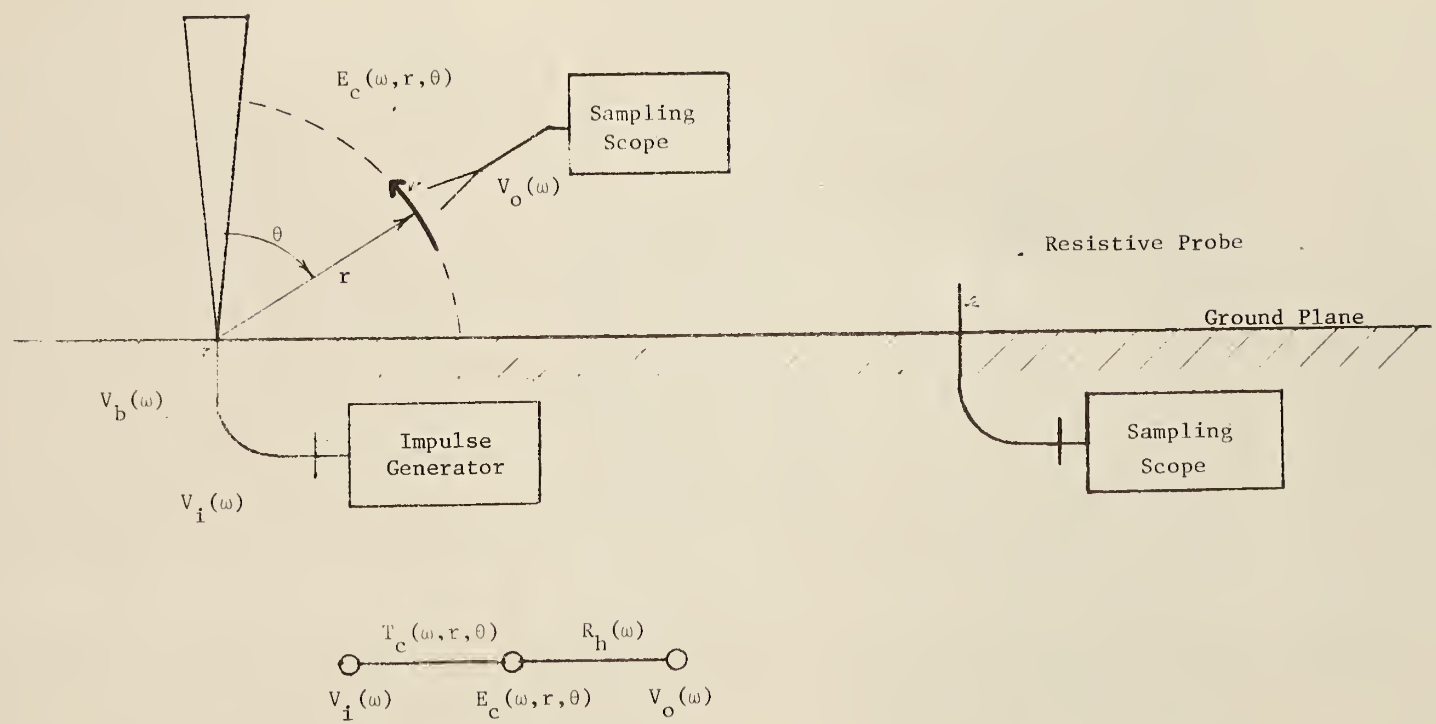

Figure 1. Measurement of R_{h1}.

Many studies have been made of broadband antennas. These have consisted of theoretical analyses [1,2,3] and qualitative experimental measurements [2,3]. The parameters considered have included boresight impulse response and transfer function [2,3], time domain antenna patterns [2,3], antenna modeling with pole-zero singularities [1], and questions of reciprocity [4,5].

The consensus in much of the research on antennas for impulsive field generation has been that the so-called TEM horn is the most promising broadband antenna available. We have developed our own version of the TEM horn which we feel has the best features of and some improvements over the earlier designs. Our main effort, however, has been a quantitative evaluation of the field generation and measurement properties of the TEM horn which will enable it to be used both as a standard impulsive field generator and as a standard receiver.

In this report we use the theory that is relevant to our measurement and add some modifications which we feel make our measurements more meaningful. We then describe the measurement process that we have found most suitable to the development of a standard impulsive field and give the design procedure and results of measurements on four balanced TEM horn antennas. These antennas were constructed for use by the Army Redstone Arsenal at Huntsville, Alabama, and for further study at NBS. A resistive monopole developed here at NBS was used as part of the evaluation and is described herein.

2. FIELD MEASUREMENT EQUATIONS

We now derive two independent ways of rapidly measuring the boresight receiving characteristics of antennas like the TEM horn over a broad frequency range. These two methods are compared and an error expression developed. The transmitting characteristics of the TEM horn is given. As a result, it is possible to use these horns either as sources of standard fields or as standard receivers.

The first method of measuring the receiving function is illustrated schematically in figure 1 together with the appropriate signal flow diagram where $V_i(\omega)$ and $V_o(\omega)$ are the input and output voltages, respectively, and $E_c\ (\omega,r,\theta)$ is the electric field generated by a conical transmission line at the location, r,θ of the horn. In this measurement the resistive probe is not present. T_c and R_h are defined by the equations below, and the subscripts c and h denote properties of the cone and horn antennas respectively.

$$E_c(\omega,r,\theta) = T_c(\omega,r,\theta)\ V_i(\omega) \qquad (1)$$

$$V_o(\omega) = R_h(\omega)\ E_c(\omega,r,\theta). \qquad (2)$$

The symbols T and R are used here instead of H that some other authors use since T and R are not transfer functions in the usual dimensionless input-output sense. Henceforth, for simplicity of notation, the functional dependence on ω, r, and θ will be understood but not explicitly written, and output input voltage ratios will be written as

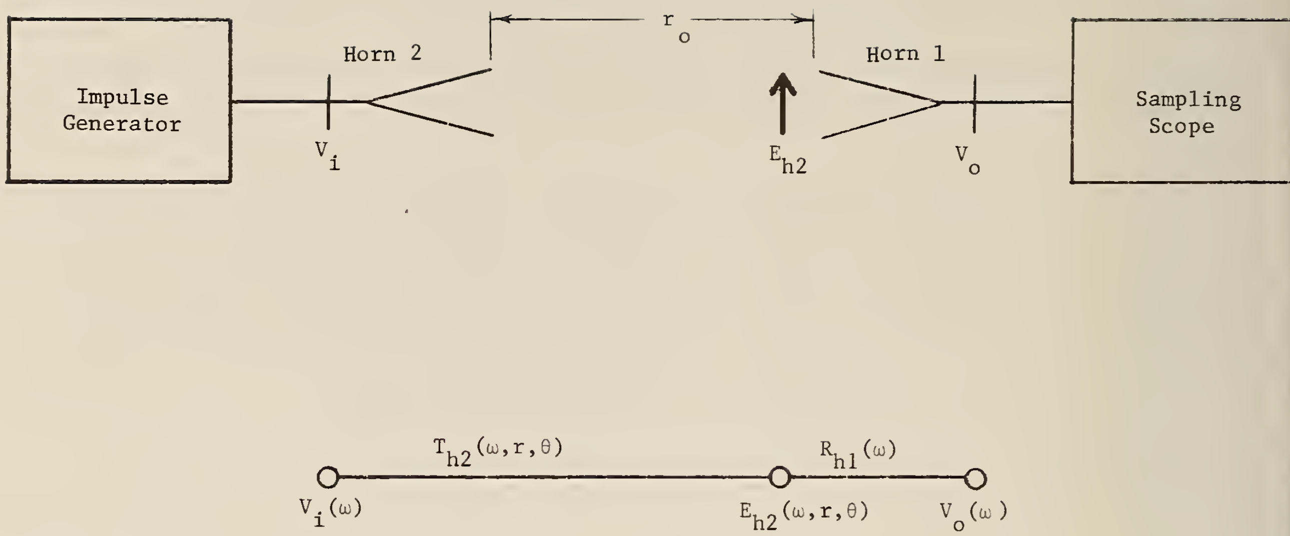

Figure 2. Measurement of T_{h2}.

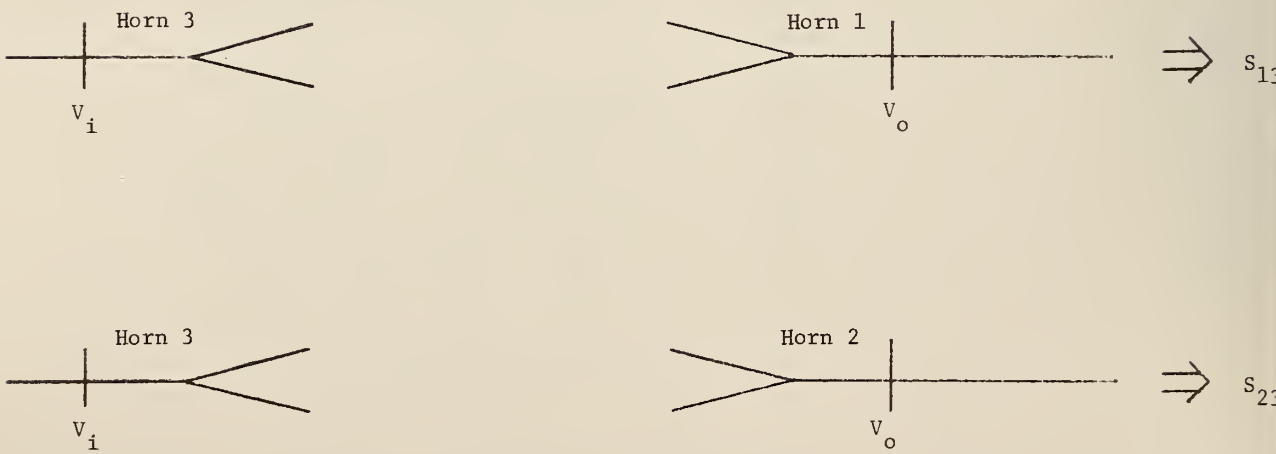

Figure 3. Measurement of R_{h1}/R_{h2}.

$$S_{hc} = V_o(\omega)(\text{from horn})/V_i(\omega)(\text{to cone})$$

when transmitting from the cone to the horn, for example. Therefore inserting eq. (1) and the definition of S_{hc} in eq. (2) and solving for R_h,

$$R_h = \frac{1}{T_c} S_{hc}. \tag{3}$$

Therefore, to measure the receiving function of the horn, one must measure the transfer function of the cone horn combination S_{hc} and divide by the cone transmitting function T_c. The quantity T_c is defined by the usual expression for the field in a conical transmission line [6] as outlined in section 4.1, Standard Cone Antenna, and the measurement of S_{hc} is described in section 3, Measurement System.

An independent way of measuring the horn receive function is obtained with two nominally identical horns as shown in figure 2, with the appropriate signal flow diagram. This second determination will be denoted R'_{h1}. The subscripts h1 and h2 refer to horns 1 and 2 respectively. The separation between the apertures of the two horns is $r = r_o$ and for simplicity, only on-axis gain will be calculated. For this arrangement

$$E_{h2} = T_{h2} V_i \tag{4}$$

and

$$V_o = R'_{h1} E_{h2}. \tag{5}$$

Therefore, with eq. (4) in eq. (5) and solving for R'_{h1}, one has

$$R'_{h1} = \frac{1}{T_{h2}} S_{12} \tag{6a}$$

where S_{12} is an abbreviation for S_{h1h2}. Solving for T_{h2},

$$T_{h2} = \frac{1}{R'_{h1}} S_{12}. \tag{6b}$$

In appendix A it is shown that the far field, on-axis expression for T_{h2} is given by,

$$T_{h2} = \frac{-i\eta}{Z_o \lambda r_o} R_{h2} e^{ikr_o} \tag{7}$$

where η is the impedance of free space, Z_o is the characteristic impedance of the coaxial waveguide that feeds the antenna, assumed to be real and frequency independent, (and also across which V_o appears), λ is the wavelength of the radiation and equals $\frac{2\pi}{\omega}$ times the velocity of light, and $k = 2\pi/\lambda$. This expression is equivalent in the time domain to the transmitting function being the derivative of the receiving function [4,5]. The validity of this relation was verified using a resistively loaded monopole which will be described later.

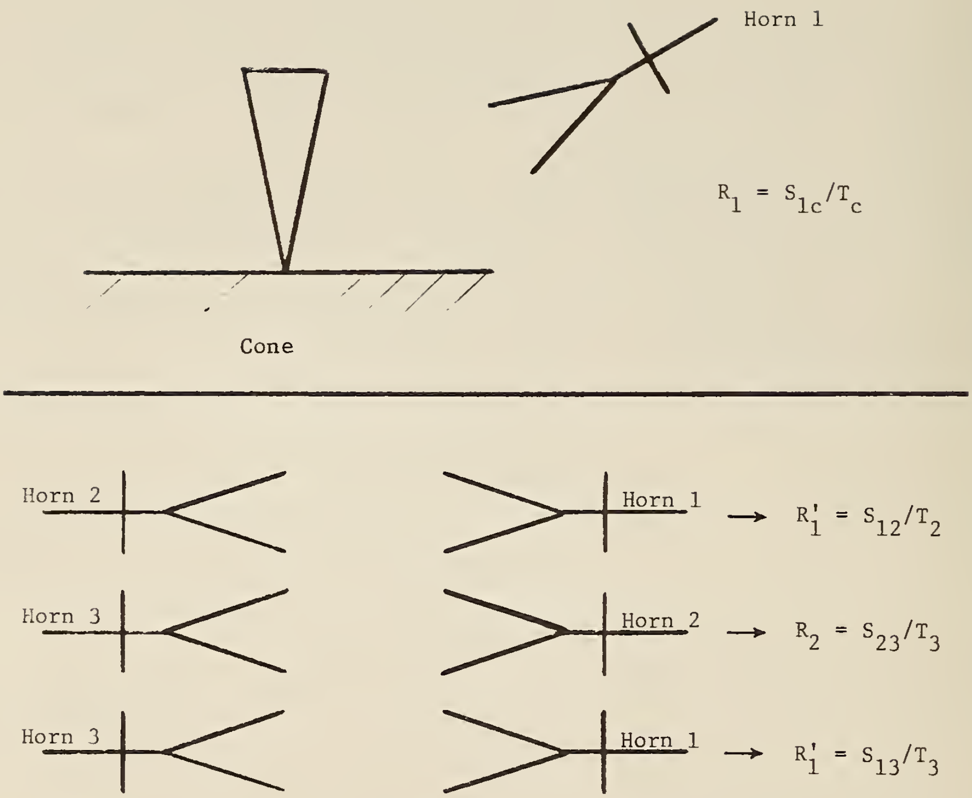

Figure 4. Two independent measurements of R_{h1}.

Therefore, substituting eq. (7) in eq. (6a)

$$R_{h1}'^{\,2} = \frac{iZ_o\lambda r_o}{\eta}\left(\frac{R_{h1}'}{R_{h2}}\right) S_{12}\, e^{-ikr_o} \tag{8}$$

The ratio, $\frac{R_{h1}'}{R_{h2}}$ can be determined with a third antenna which we will take to be a horn antenna for simplicity. The measurement setup is shown schematically in figure 3. In the first measurement only horn 3 and 1 are present, and the voltage ratio, S_{13}, is measured. In the second measurement horn 1 is replaced by horn 2 in as closely the same position as possible, and the voltage ratio, S_{23}, is measured. Substituting these results in eq. (8) and taking the square root yields,

$$R_{h1}' = \left(\frac{iZ_o}{\eta}\lambda r_o \frac{S_{13}S_{12}}{S_{23}}\right)^{1/2} e^{-\frac{ikr_o}{2}} \tag{9}$$

This then is an independent determination of the horn receiving function and can be compared with that obtained using the calculated field of the cone. The comparison is summarized in figure 4.

Having once determined R_{h1}, one can determine R_{h2} from the ratio used in eq. (8) and then using either eq. (6b) or eq. (7), one can determine T_{h2} and T_{h1}. Having determined these parameters, eqs. (1), (2), (4), and (5) can be used to determine the desired electric field quantities. The above analysis was performed for TEM horn antennas, but it need not be restricted to TEM horn antennas.

If desired, the emphasis of the above measurements could be rearranged to get independent determinations of the cone transmission function, one determination would be theoretical and the other would be experimental using parameters determined according to figure 4 with R_{h1} determined as in the bottom half of figure 4.

The uncertainty in the determination of R_h, δR_h, by the two methods, can be found by taking the derivative of eqs. (3) and (9) with the result that,

$$\frac{\delta R_{hi}}{R_{h1}} = -\frac{\delta T_c}{T_c} + \frac{\delta S_{hc}}{S_{hc}} \tag{10a}$$

and

$$\frac{\delta R_{h1}'}{R_{h1}'} = \frac{1}{2}\left(\frac{\delta S_{13}}{S_{13}} + \frac{\delta S_{12}}{S_{12}} - \frac{\delta S_{23}}{S_{23}} + \left(\frac{1}{r_o}+ik\right)\delta r_o\right) \tag{10b}$$

where errors in η, Z_o, and λ have been assumed negligibly small. By careful definition of the horn aperture plane, δr_o may also be negligible. Additional sources of error may be present due to near-field or off-axis effects which are not included in eq. (10), and will be considered later. In any event, a conservative least upper bound on the measurement error is the simple sum of all the individual voltage measurement errors, etc. However, when determining the radiated field strength, the error in measuring the absolute voltage

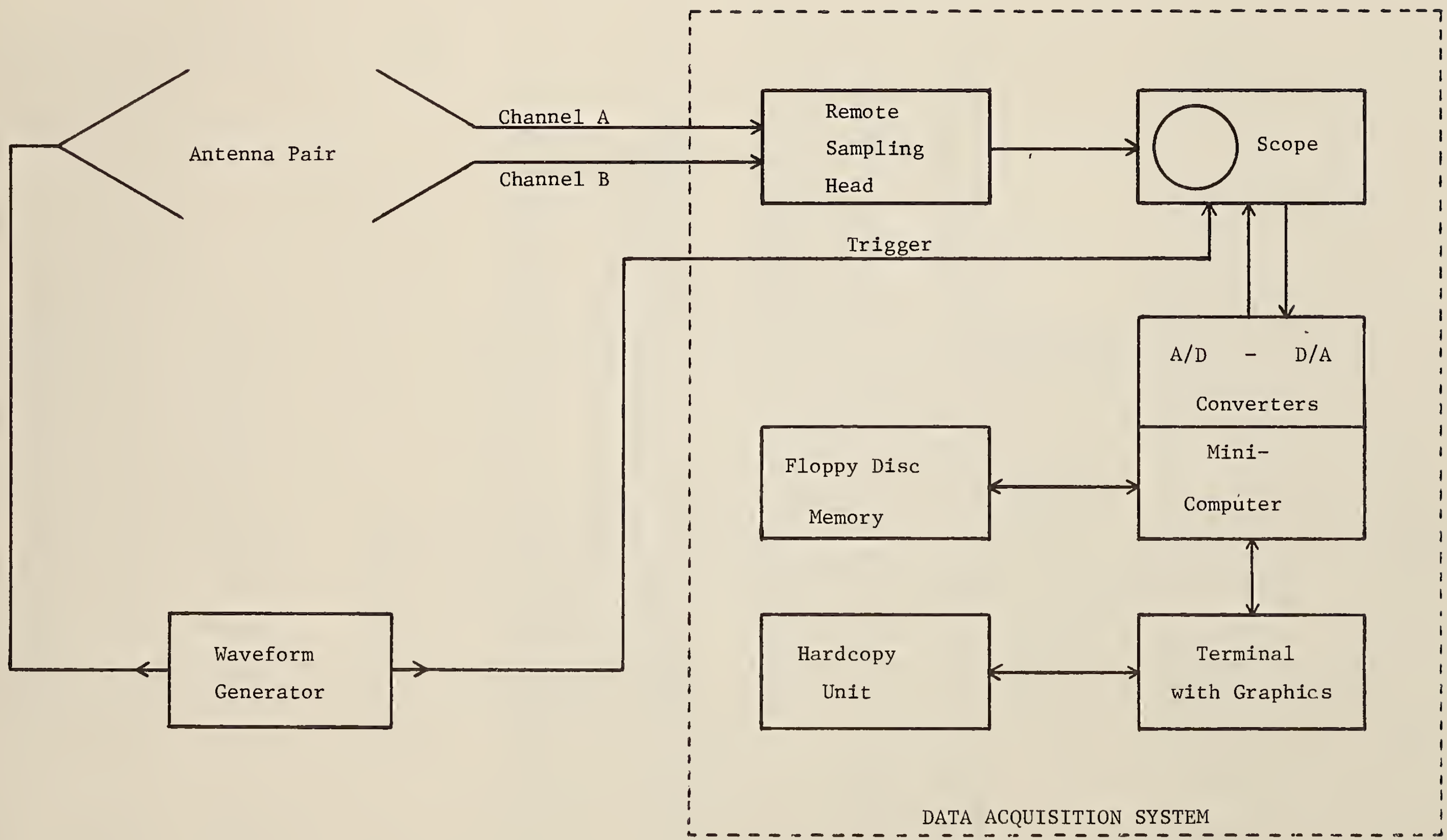

Figure 5. Antenna measurement system.

level versus time and consequently versus frequency must be determined and added to the above error bound. An estimate of these errors can be found in section 6.2 of this report, but a complete measurement of these error limits will be the subject of a future report.

3. MEASUREMENT SYSTEM

The basic measurement system as shown in figure 5 is the same for each of the various antenna combinations mentioned in the previous section. Figure 5 shows the transmitting antenna being excited by a time domain waveform generator. The signal used can be a step function, an impulse, or a variety of pulse shapes.

For calibrations on the ground plane, the antennas consist of a standard transmitting cone with a resistive probe or TEM horn receiver. For measurements in a free-space field, not associated with the ground plane, combinations of horns are used for both transmitting and receiving.

The receiver is a sampling oscilloscope with a 50 ohm input impedance and a bandwidth of dc to 18 GHz which was modified to interface with a minicomputer. The scope-computer combination called the Automatic Pulse Measurement System (APMS) has been described by Andrews and Gans [7,8,9]. The oscilloscope is a sampling device and requires that the input be repetitive.

The operation of the oscilloscope is directly controlled by the minicomputer, except for the time synchronization which comes from the generator. The computer determines the sampling point, accepts the analog signal from the scope and digitizes it, moves the sampling point to a new place on the waveform, and then arms the sweep circuits to be ready for a trigger from the generator. The D/A and A/D converters in the computer are 12-bit devices, and this is one factor that limits the resolution of the measurement and determines the types of waveforms that can be measured.

After the data has been stored in memory, the computer is free to manipulate it under program control. One program presently available is the Fast Fourier Transform (FFT) which converts the time domain data to frequency domain information. A time domain waveform is measured by the system before it is transmitted, and the FFT is used to convert it to frequency domain information. A similar measurement is made on the signal after it is transmitted and received again. The attenuation and phase delay of the transmitting and receiving antennas together is then equal to the transformed received signal divided by the transformed transmitted signal. This determines the quantity S_{hc} of eq. (3), for example.

Other programs are being developed to remove the effects of reflections which occur in the environment around the antennas and to make the ground plane appear to be larger than it actually is. One program makes use of homomorphic deconvolution to remove reflections [10]; a second program is based on the Singularity Expansion Method, i.e., finding the poles of an antenna system.

The various parts of the measurement system will now be discussed in greater detail. Since the APMS presents some basic limitations on the type of waveforms it can measure, the antennas and generator were designed to be compatible with the measuring system.

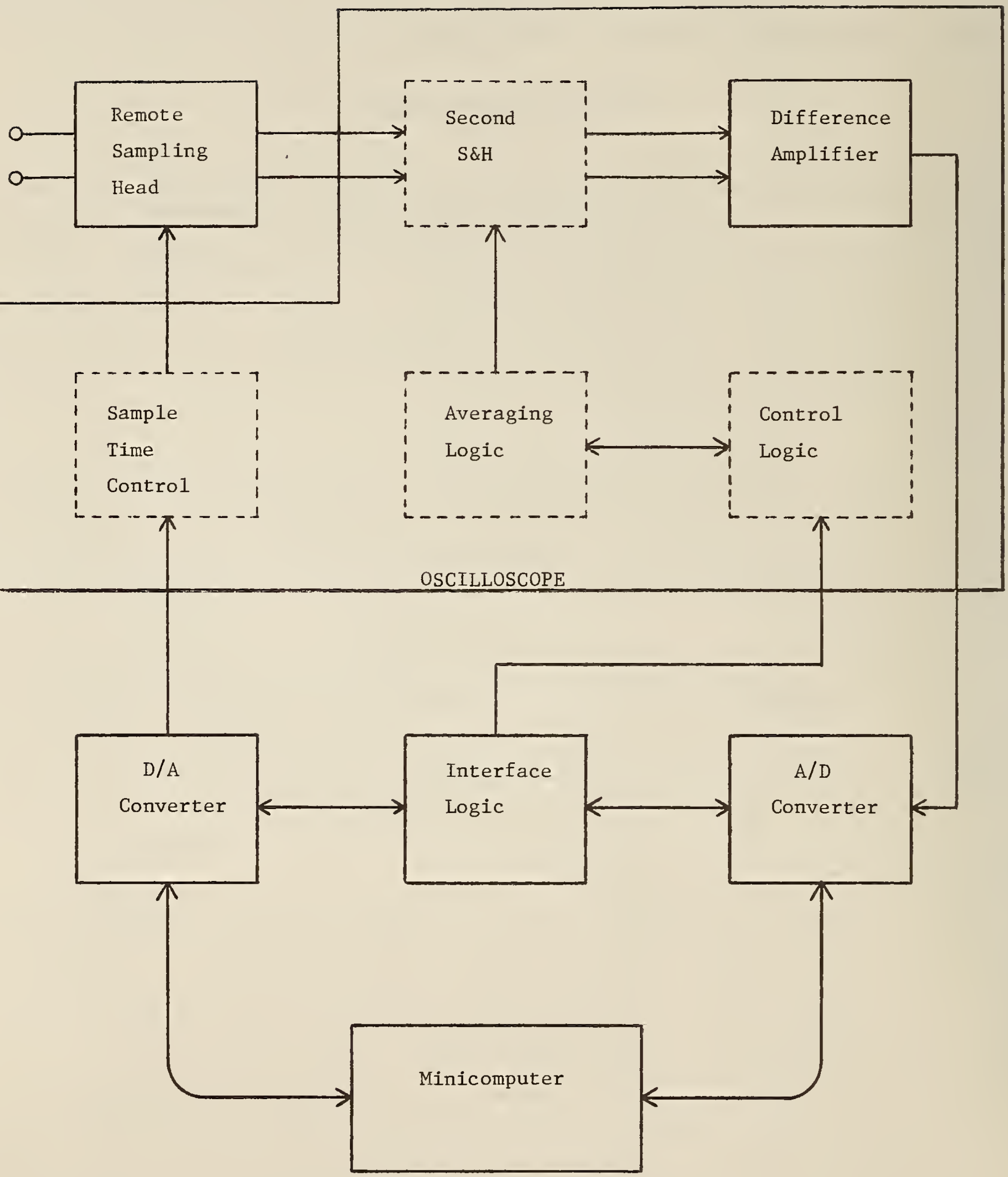

Figure 6. Sampling scope - computer modifications.

3.1. Sampling Oscilloscope

The oscilloscope was modified specifically for antenna measurement use as shown in figure 6. The solid blocks are original parts of the scope, dashed blocks are new parts or changes.

The remote dual channel sampling head made it possible to sample directly at the output port (or ports) of the receiving antenna without having large pieces of equipment in the vicinity to distort the fields. The short duration signals are sampled and stretched in the sampling head, and the narrow bandwidth signals which result are sent to the oscilloscope plug-in through 3 meters (10 ft) of cable. The time at which the sample is taken is a function of the time of arrival of a trigger from the signal generator and a variable delay in the oscilloscope controlled by the computer.

A second sample and hold stage is contained in the plug-in to the scope and usually further stretches the input analog signal in time so that it can be used to vertically locate a single dot on the CRT. In the unmodified form of the oscilloscope, each sample produces one dot after another on the CRT face and the whole pattern is just this sequence of dots with appropriate vertical deflections. In the modified unit, the oscilloscope hardware can take repeated samples at the same time location of the waveform, and the second sample and hold stage is used to sum up all these inputs. Averages of 1, 10, or 100 are possible.

After the correct average is taken at one location of the input waveshape, the computer can either change the delay time of the sampler to measure a new part of the input waveshape or request a repeat of the previous measurement for digital averaging. Since the input signals are quite small, this averaging can produce the improvement in signal to noise ratio required for typical antenna measurements. The noise reduction permits the signal to be displayed directly on the CRT without having to be processed by the computer. This allows the operator to find received signals that might be buried in the noise in real time. The analog signal is then processed by the computer's A/D converter, and the information is stored in the core memory of the computer. The maximum rate of the computer's A/D conversions is about 25 kHz.

Each scope channel is averaged separately and then can be combined as A + B or A - B before being digitized. When antennas are measured on the ground plane, signals are measured with respect to ground using only one 50 ohm coaxial input, either channel A or B. Antennas designed for free-space field measurements, that is measurements that are not referenced to a ground plane, are balanced, and the two output signals are 180 degrees out of phase. These are measured by applying one to channel A, the other to channel B, and measuring the difference in the outputs of the two channels (A-B). This presupposes that the two channels are matched in gain and phase which is the case at the frequencies being used.

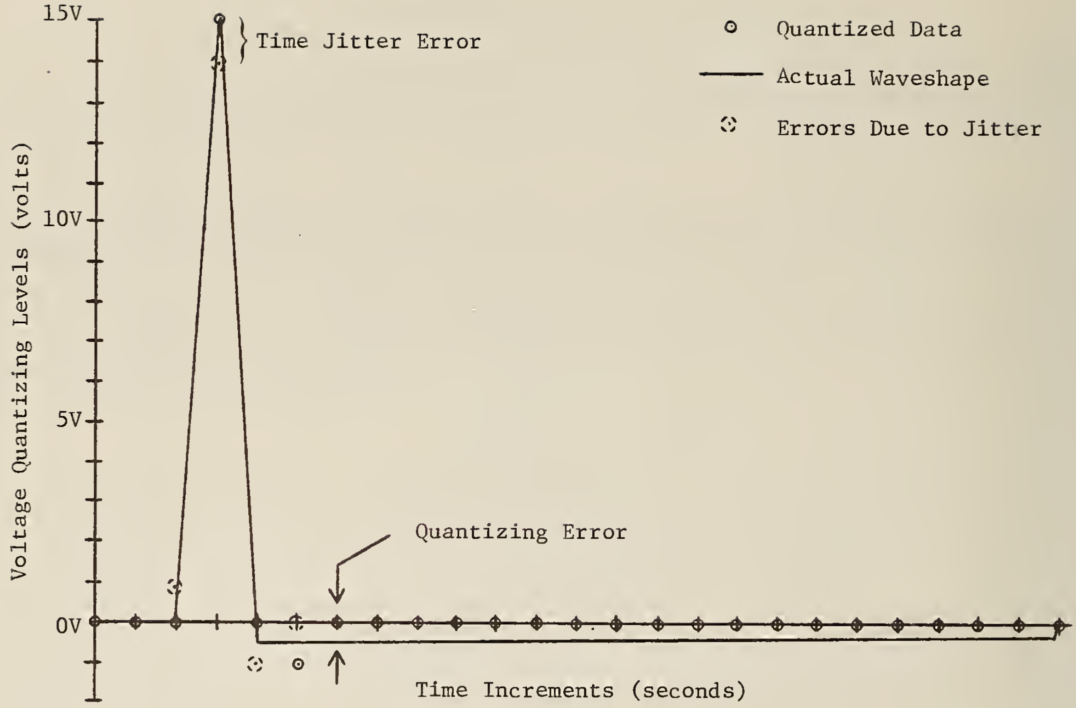

Figure 7. Quantizing and jitter errors.

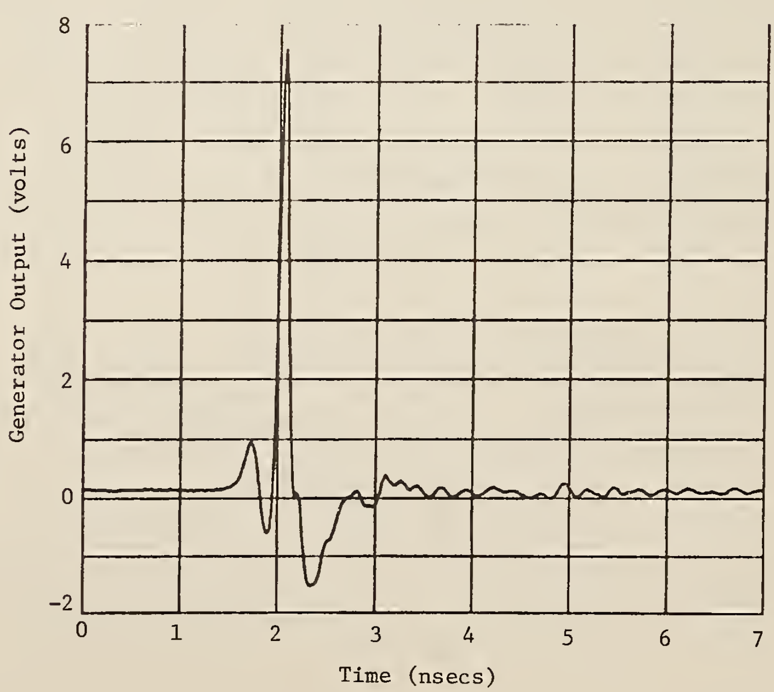

Figure 8. Driving impulse to the transmitting antenna.

3.2 Computer, Peripherals, and Analog Converters

The minicomputer used in the system was slightly modified to interface with the oscilloscope logic as mentioned in [7]. It was a commercially available unit with internal 12-bit A/D and D/A converters.

The peripherals needed with the computer are shown in figure 5. The terminal has a graphics capability, and a fast hard copy device is also necessary. Most programs and data files used during a measurement are large and the additional memory of a floppy disc is needed to handle this volume. A detailed description of the peripherals will not be given here since they do not directly effect the accuracy of the measurements, assuming that they function properly.

Since the sample time position is controlled by the computer's D/A converter, the number of samples taken in the measurement time window is a function of the number of discrete voltage levels which the converter can produce. A 10-bit converter has 1024 discrete levels and could produce that many different delays, each sample point being separated from the next by only one bit of information. If the accuracy of the converter were ± 1/2 bit, the separation between adjacent samples might vary from zero to twice the intended size, giving rise to rather large errors. For this reason, a 1024 point sample sequence is better produced by a 12-bit or preferably 14-bit D/A converter. The 12-bit converter available in the minicomputer provides a sample density of 1024 points per trace with an adequate accuracy, but this becomes the major limitation on the type of waveforms that can be analyzed, since the error in time can cause a large error in amplitude when the slope of the waveform is large.

In order to make a correct measurement, the entire waveform must be sampled, that is, it must fit in the measurement window. Consider a waveshape composed of a fast transition followed much later by a significant reflection. In order to record both the initial response and the reflection in the same time window, the sweep speed may have to be slowed, allowing the possiblity that the transition itself is too fast for the sampler to generate an adequate number of samples during the transition time. For antennas having this characteristic, error in the measurement can be large.

A second type of measurement error occurs if the waveform has a component with a very small amplitude but lasting for a long time. The energy is appreciable and will contribute significantly to the spectrum but may go undetected by the sampler because its amplitude at any one point in time is not large enough to move the A/D converter from one quantizing level to the next.

Some impulse generators produce a waveform like that of figure 7. If the impulse is 15 volts high and 2 samples wide, the area under the impulse curve equals

$$\frac{1}{2} \times 15 \times 2 = 15 \text{ volt seconds.}$$

The impulse is followed by a negative undershoot that has an area equal to 1/3 the area under the impulse but has a small amplitude. It is possible that the digitized data would miss the undershoot entirely.

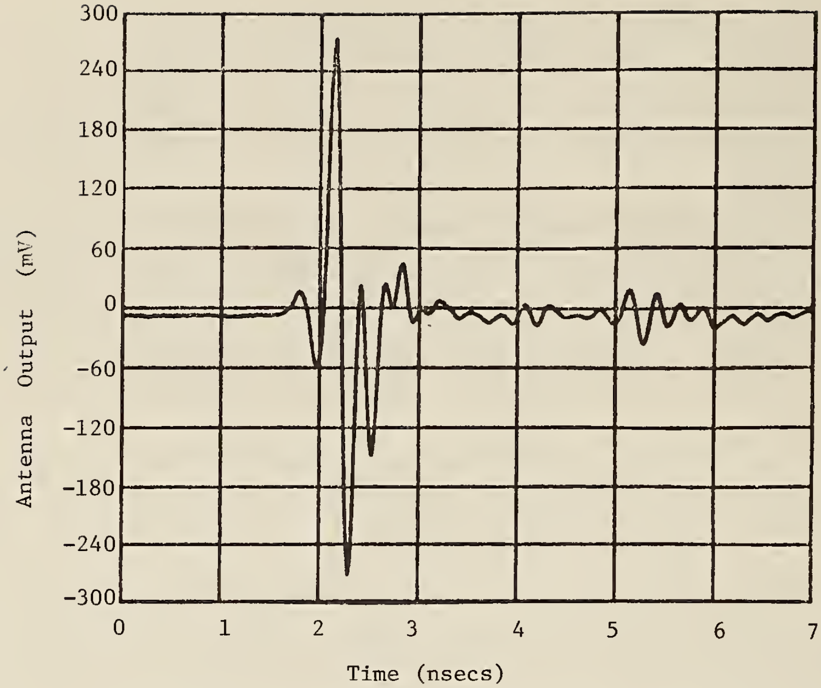

Figure 9. Output voltage from receiving antenna.

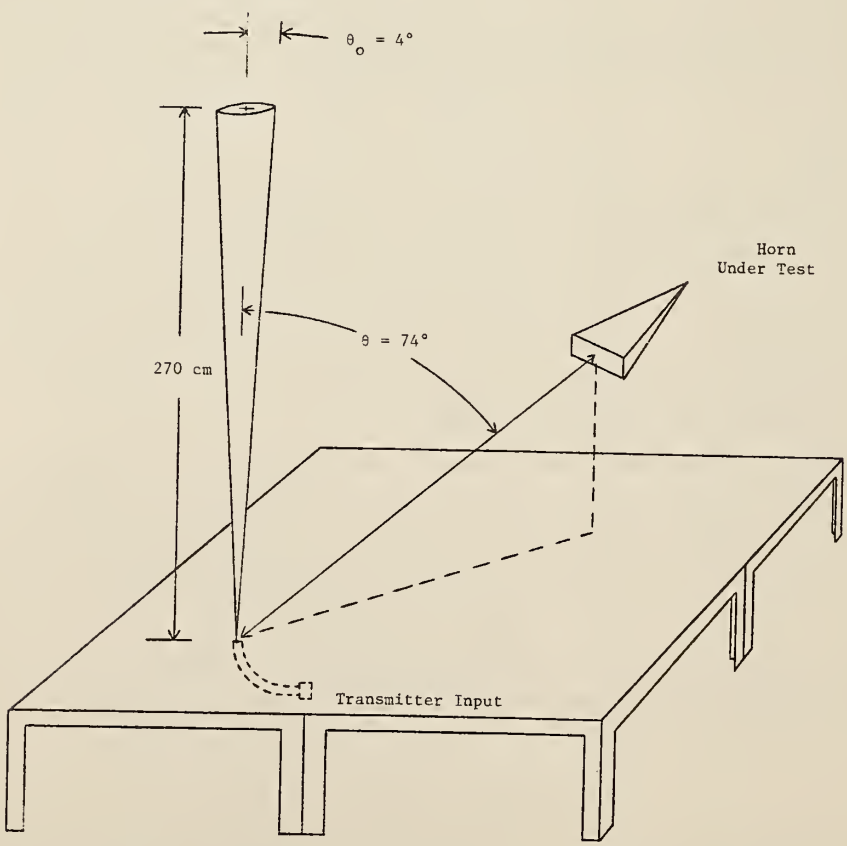

Figure 10. Standard field from cone antenna.

With 12-bit A/D and D/A converters, the vertical and horizontal scales are divided into 4096 discrete digitizing levels. As a rule of thumb, in this case, the waveshape should occupy more than half the vertical space of the CRT and should be completely finished in a time not to exceed 300 times the duration of the fastest transition to be recorded. It is desirable that the undershoot end within a few pulse durations. The impulse waveform used in our measurements is shown in figure 8 and can be seen to be finished in a time less than 25 times the risetime. The received output of a pair of TEM horns built for the Army Redstone Arsenal is shown in figure 9 and has an internal reflection which occurs 3 ns after the main response. The total response is finished in about 80 times the risetime. Both the main response and the reflection are easily measured by the APMS. An additional refection occurs as an interaction between the horn and balun which occurs 12 ns after the major response but is not recorded in the time window. This could be measured on the APMS except, for this large a time, other reflections within the measurement environment interfere.

4. ANTENNA SYSTEMS

4.1. Standard Cone Antenna

The conical antenna was chosen as a standard to provide a reference measurement system that is better defined theoretically than the TEM horn, and therefore whose accuracy can be determined more completely. Figure 10 is a schematic of the cone located over a ground plane, and figure 11 is a photograph of the 270 cm (8.9 ft) long cone over an early version of the ground plane and showing the APMS in the background.

The cone is driven from a generator with a 50 ohm resistive source impedance. The impulsive signal is brought up from under the ground plane on a 3 mm semi-rigid 50 Ω coax line and propagates out along the cone forming a spherically expanding wave of short duration. For a length of time less than the propagation time along the cone, the conical antenna presents a constant resistive impedance to the expanding electromagnetic wave throughout its entire length and looks exactly like a biconical transmission line. In effect, the energy propagating from the 50 ohm line simply sees a resistive mismatch at the base of the cone, and the two form a frequency insensitive voltage divider without introducing waveform distortion to the time domain waveform. The field can then be described as an attenuated replica of the driving voltage.

The impedance of the cone over a ground plane is a function only of the cone half angle (θ_o) which is chosen at 4° for ease of fabrication. Smaller angles produce too long and thin a point while larger angles produce too large a disc at the top end. The characteristic impedance is given by [6]

$$Z_o = 60 \ln \cot (\theta_o/2). \tag{11}$$

Figure 11. Cone antenna on the ground plane.

If $\theta_o = 4$ degrees, the characteristic impedance (Z_o) becomes approximately 200 ohms. Figure 12 shows a TDR measurement of the cone indicating that its impedance is close to 200 ohms.

Knowing the impedance of the cone and the fact that it is resistive, allows a simple calculation of the voltage applied to the cone. A direct measurement of the output from an impulse generator is usually made with an oscilloscope having a 50 Ω input impedance and yields

$$V_{gen}(t) = \frac{V(t)_{meas.} (R_{gen} + 50)}{50} . \quad (12)$$

The voltage appearing on the cone with respect to the ground plane is

$$V_{cone}(t) = \frac{V_{gen}(t) \quad 200}{R_{gen} + 200} . \quad (13)$$

Substituting eq. (12) into (13) gives

$$V_{cone}(t) = \frac{4V(t)_{meas} (R_{gen} + 50)}{R_{gen} + 200} . \quad (14)$$

Special care has been taken to ensure that the NBS built generators have a 50 ohm impedance over the frequency range of interest, and in this case eq. (14) reduces simply to

$$V(t)_{cone} = 1.60 \, V(t)_{meas.} . \quad (15)$$

Given the voltage between cone and ground plane as a function of time, the field in the TEM mode at a point in space can also be given as a function of time. From [6] for a <u>biconical</u> transmission line in the <u>frequency</u> domain,

$$rE_\theta(\omega) = \frac{\eta}{\sin\theta}\left(Ae^{i(\omega t-kr)} + Be^{i(\omega t+kr)}\right) \quad (16)$$

and the voltage between the pair of cones is given as

$$V(\omega) = 2\eta \ln\left(\cot\frac{\theta_o}{2}\right)\left(Ae^{i(\omega t-kr)} + Be^{i(\omega t+kr)}\right). \quad (17)$$

Substituting (17) into (16) and $V_{cone}(\omega) = V(\omega)/2$(over a ground plane),

$$E_\theta(\omega) = \frac{V_{cone}(\omega)}{r \sin(\theta) \ln\left(\cot\frac{\theta_o}{2}\right)} \quad (18)$$

or in the time domain

$$E_\theta(r,\theta,t) = \frac{V_{cone}(t)}{r(\sin\theta) \ln\left(\cot\frac{\theta_o}{2}\right)} \quad (19)$$

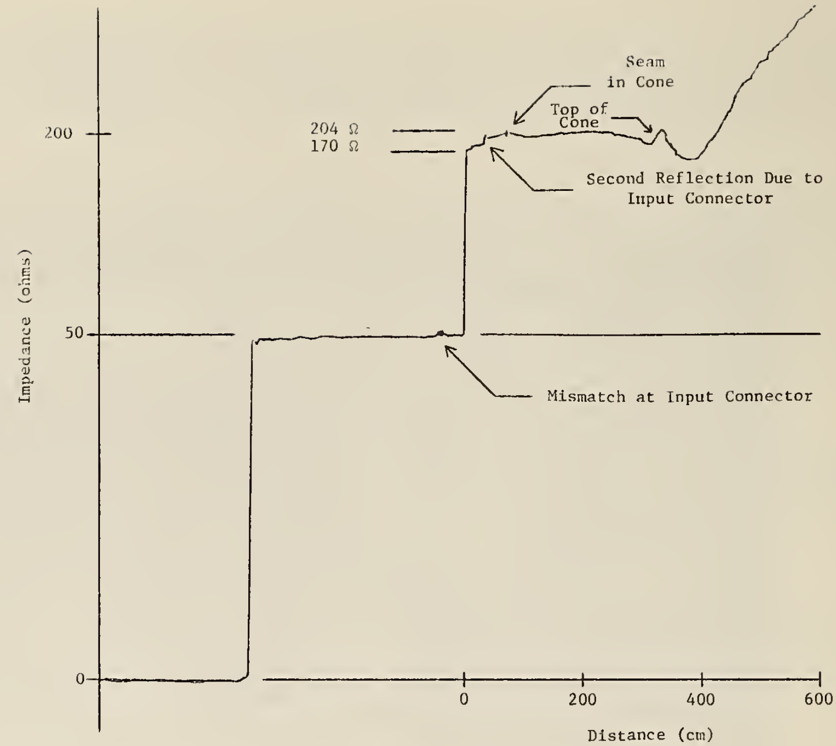

Figure 12. TDR trace of conical antenna.

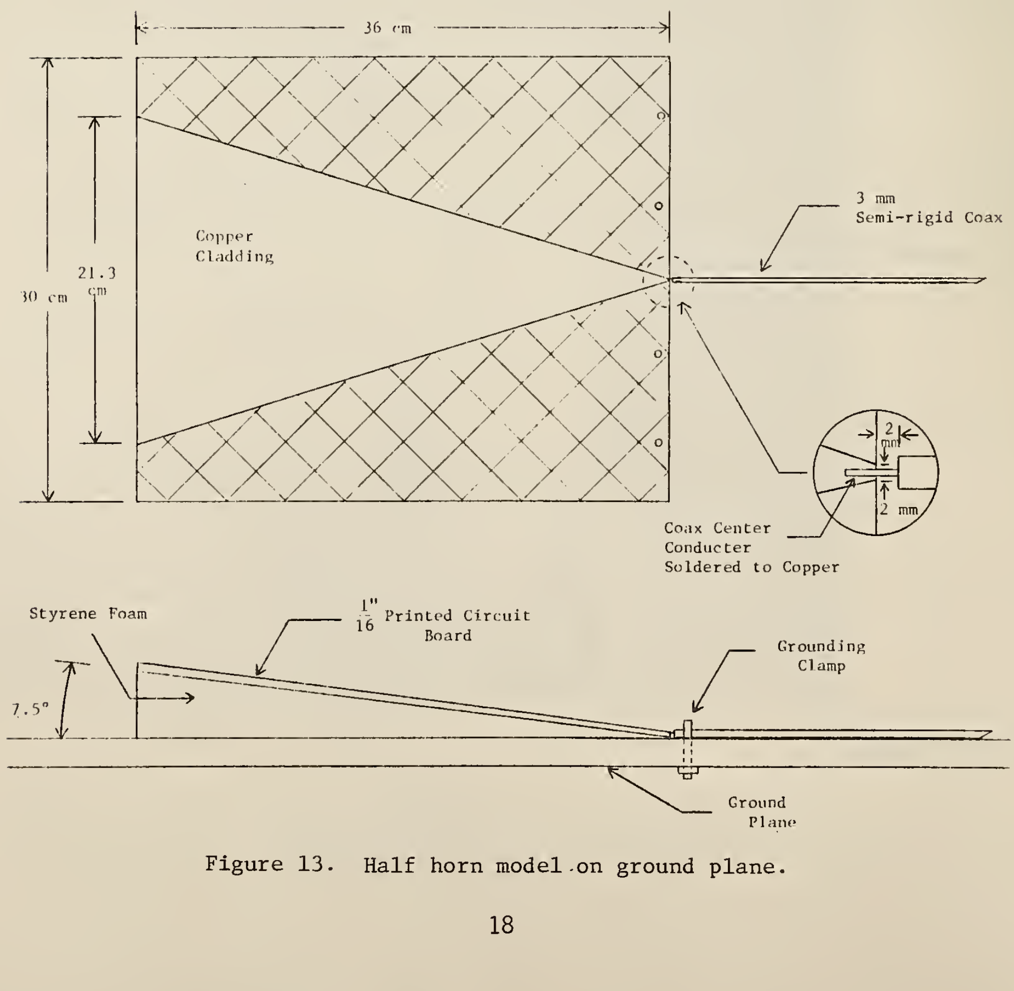

Figure 13. Half horn model on ground plane.

where,

$E_\theta(r,\theta,t)$ is the E field as a function of time in the θ direction and at a distance r from the apex of the cone,

$V_{cone}(t)$ is the voltage between a reference point on the cone and the ground plane measured along the E field,

r is the radial distance from the apex of the cone at the ground plane to the point in space at which the field is desired,

θ is the angle between the axis of the cone and the radius r,

θ_o is the half angle of the cone.

The most important observation to make at this point is that the E field has exactly the same shape in time as the driving voltage from the impulse generator. In other words, the cone produces a field which is a high fidelity replica in time of the driving voltage. A high fidelity receiving antenna would then produce an output voltage time waveform which nearly resembles the generator time waveform, and this is used as a test for the quality of the antenna.

4.2 TEM Horn Antenna

The antennas chosen for the impulsive free-space field measurements (not on the ground plane) were the TEM horns as mentioned previously. Besides being mechanically rugged, they are quite broadband in the receiving mode, both in magnitude and phase.

A half-horn was constructed as shown in figure 13. The antenna was made by cutting the proper triangular shape into the copper foil on a standard 1/16" glass epoxy printed circuit board. Holes drilled on the edge of the board are used to fasten the antenna to the ground plane with 4-40 nylon bolts, and the wedge spacer was cut from polystyrene foam. The coax is again the 3 mm semi-rigid coax cable with a type N connector.

Figure 14 shows the time domain receiving response of the horn when the cone was used for transmitting. The similarity between transmitted (Fig. 8) and received impulses attests to the good fidelity of the horn as a receiver. The frequency domain response shown in figure 15 confirms that the response is reasonably flat (± 3 dB) from 200 MHz to 4 GHz. On the basis of this type of data, the TEM horn was chosen for use in free-space field measurements.

It is shown in the appendix that for any antenna the far-field transmitting response is exactly a constant times the derivative with respect to time of the receiving response. In other words, in the transmit mode, the low frequency rolloff with decreasing frequency is exactly 6 dB/octave steeper than in the receive mode. In order to verify these results, a resistive probe (monopole) with a flat receiving response was built to be used as a standard receiving antenna. The TEM horn was then tested in the transmitting mode with the resistive probe as receiver. Details of the probe construction are given in the next section. Figure 16 shows the probe output waveshape when the horn was transmitting. The doublet resembles a time derivative of the impulse driving the horn. The frequency response of the pair, figure 17, shows a rapid rolloff toward the lower frequencies. It was also

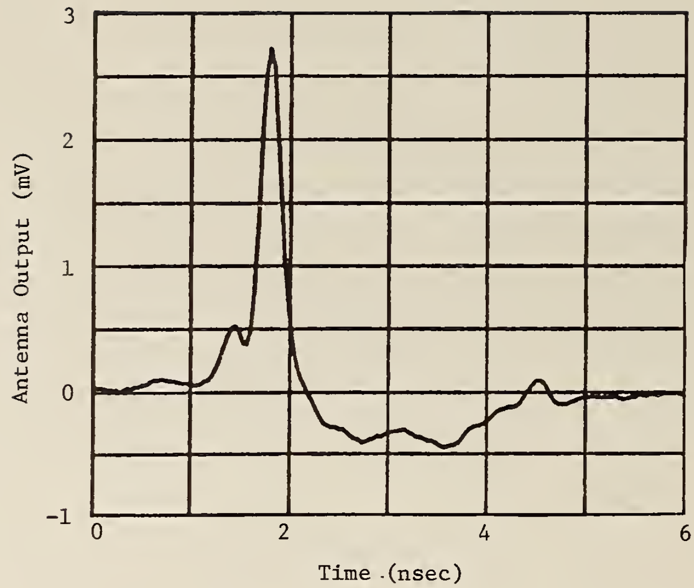

Figure 14. Receive time domain response of horn model.

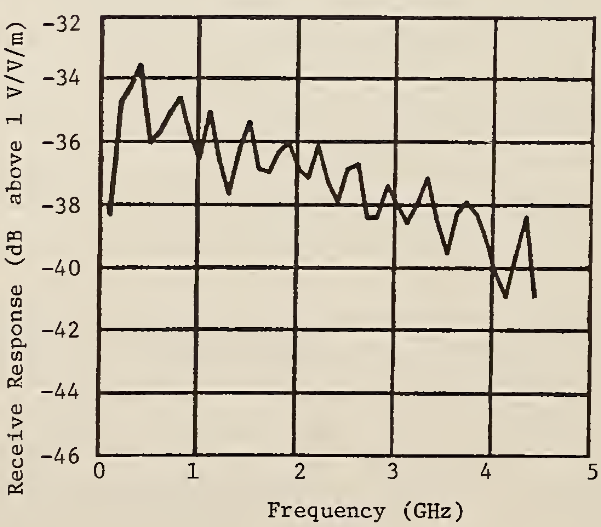

Figure 15. Receive frequency response of horn model.

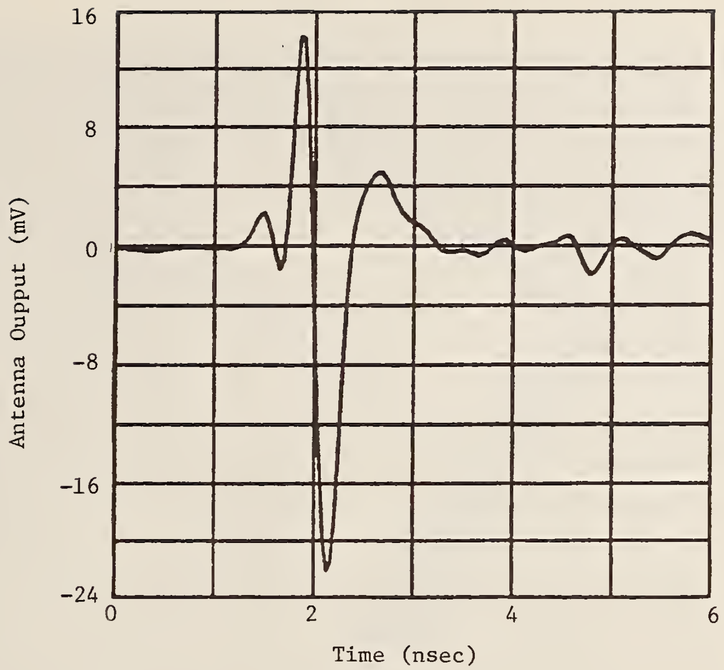

Figure 16. Time domain response of horn-resistive monopole pair.

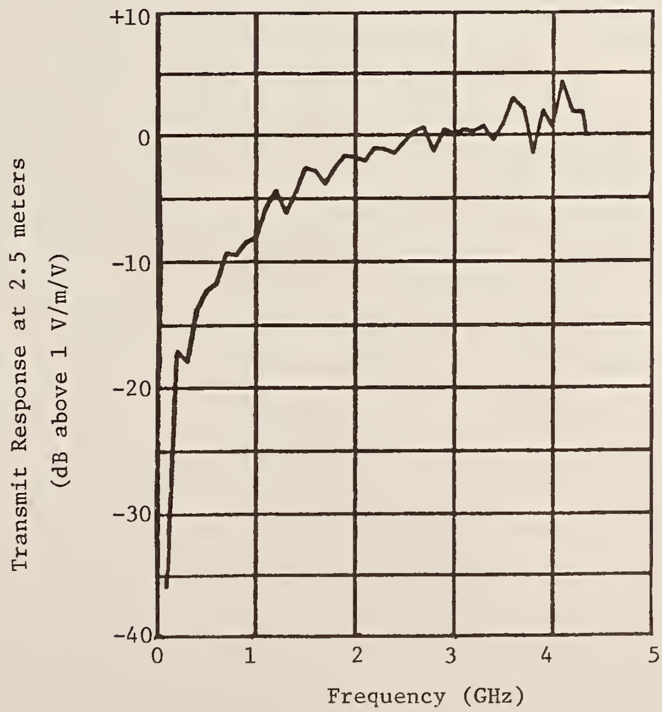

Figure 17. Frequency domain response of horn-resistive monopole pair.

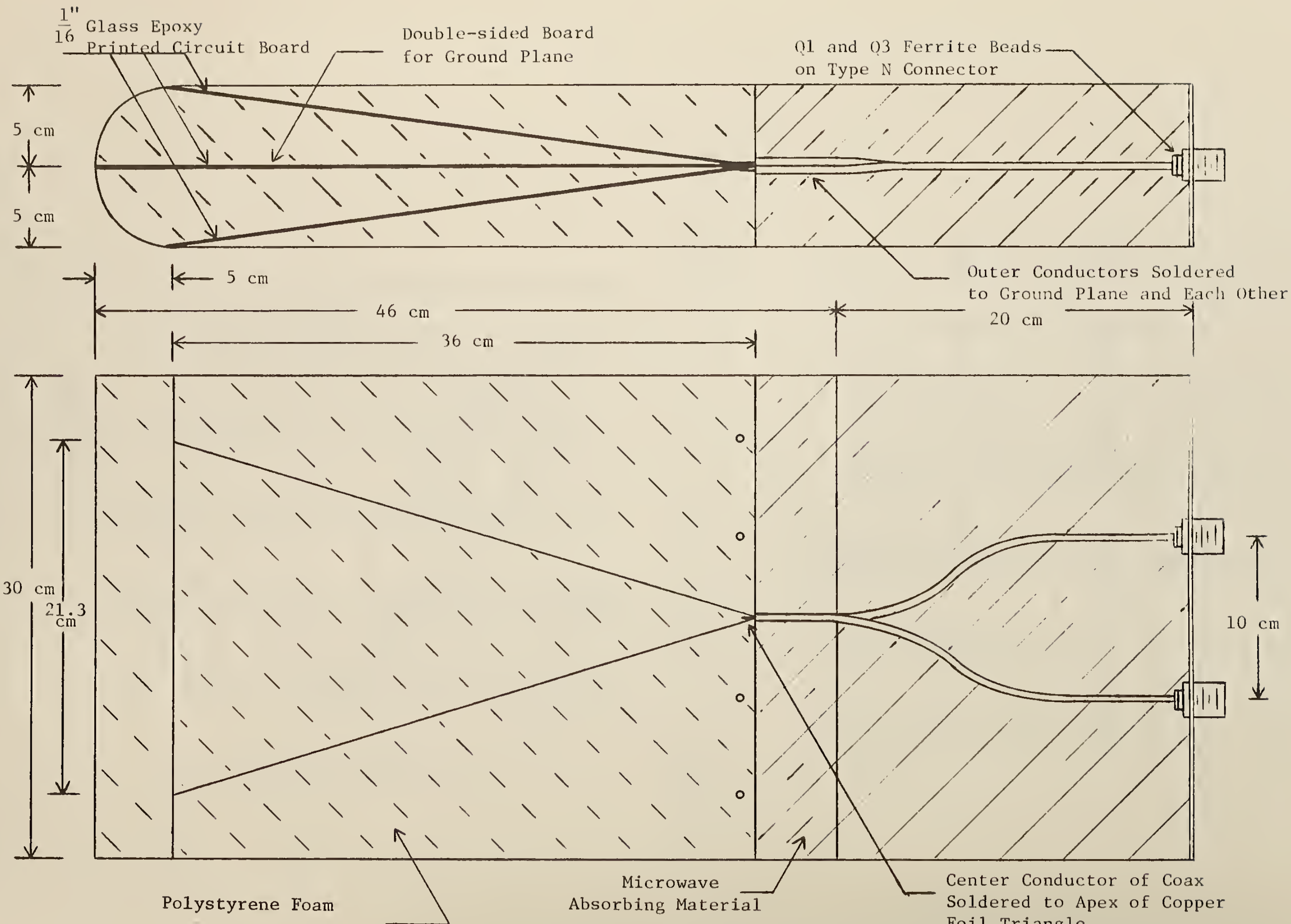

Figure 18. Horn antenna.

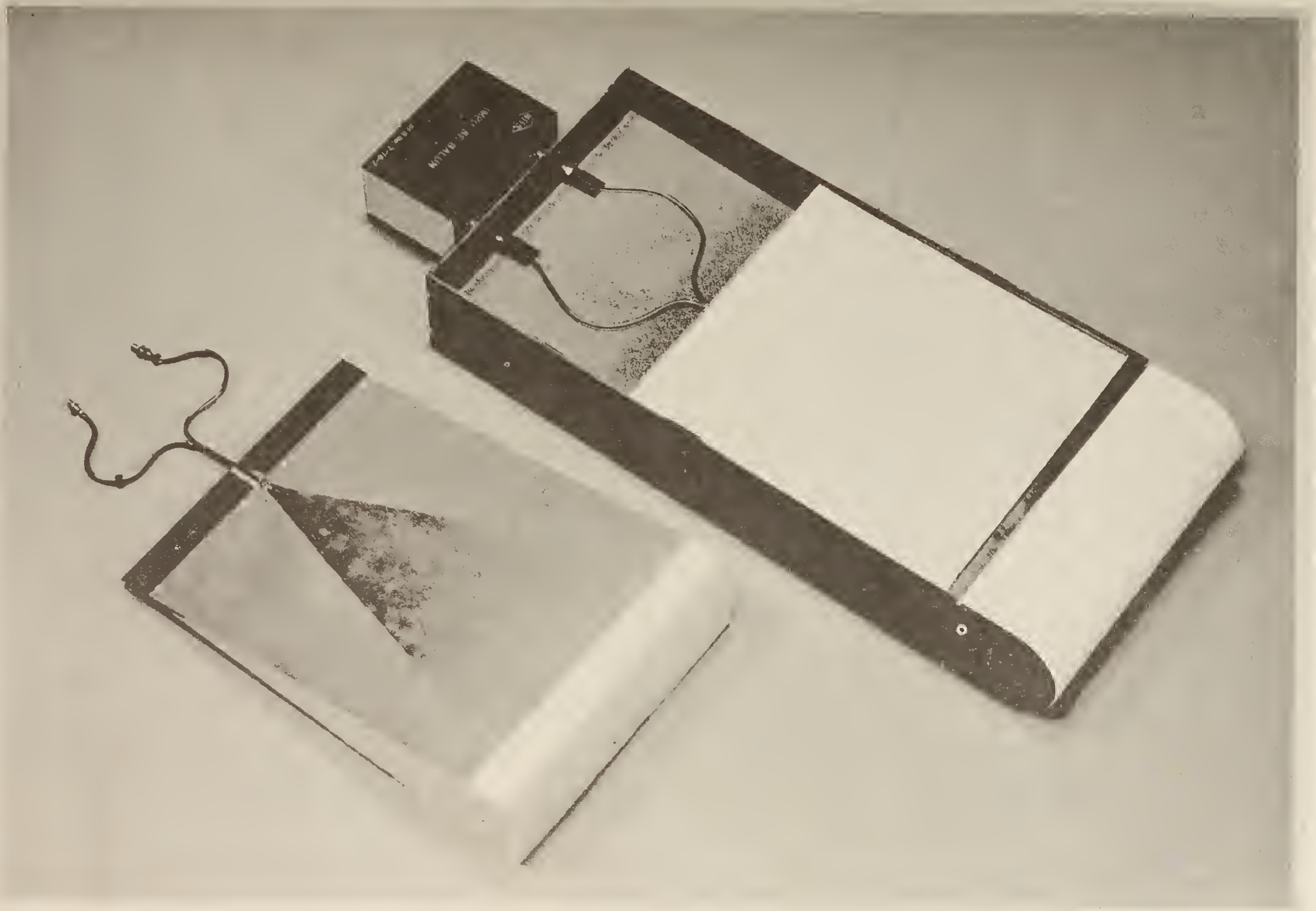

Figure 19. TEM horn construction.

shown empirically that the transmitting function of the probe was the derivative of its receiving function and the receiving function of the conical antenna was indeed the integral of its transmitting function.

TEM horns for free-space field measurements were made as nearly identical as possible to the half-horn ground plane model. A small ground plane was made a part of the horn structure to aid in making TDR impedance measurements of the horn after construction. The structure is shown schematically in figure 18. The ground plane is longer than the antenna, and has the same width as the antenna printed circuit boards. The actual antenna is shown in the photo, figure 19.

Each half of the horn is brought out separately on its own 50 ohm coax connector. This type of structure makes it easier to test each half-horn separately on a 50 ohm TDR and makes the antenna more nearly the same as the half-horn tested on the ground plane. Ferrite beads around the coax and an absorbing foam are used to damp the reflections on the ground plane that propagate onto the outer surface of the coax lines.

The antennas can then be driven through a balun which splits a single unbalanced input into two identical outputs of opposite polarity. A better way to drive the antenna would be from a balanced generator that produced the two signals directly. In the receiving mode, the two outputs can be combined in a balun. Again, the better way is to look at the two outputs directly on two channels of the sampling oscilloscope (A and B), and since they are of opposite polarity, they can be combined as A-B.

The balun is a simple broadband power divider with one output delayed and inverted while the other is simply delayed, see figure 20.

Each arm of the divider is 30 cm long, and the shields are grounded together close to the connectors. The resulting inversion joint is shown in the photograph on figure 21. The whole balun is mounted in a 7 cm x 10.5 cm x 16 cm aluminum utility box. The extra space in the box is filled with absorbing foam to reduce the effect of reflections. The time domain response is shown in figure 22 with the non-inverted output from the balun inverted in the scope for comparison with the inverted pulse. The slightly smaller wave-shape is due to the loss at the inverting splice and will have a slight degrading effect on the balance of the horn. Figure 23 shows the frequency response of a pair of identical baluns connected together in such a way that the inverted signal from one balun passes through the second without additional inversion and vice versa. In figure 24, the frequency was swept from 10 to 1200 MHz and the resultant variations are less than ± 3 dB. The ripple is caused by multiple reflections between the two baluns but the average frequency response is flat over this frequency range.

Free-space field testing of the TEM horns was done in two steps. The receiving characteristics were measured by placing the horn in the spherical field of the conical antenna but above the ground plane as shown in figure 1 and 25. Then the transfer function of a pair of horns was measured on a small laboratory range, see figure 26, where the antennas are separated by 2.5 meters and are positioned 80 cm above the floor. Results of these two measurements could then be used to determine the transmit function, T_h, and receive function, R_h, as explained in section 2.

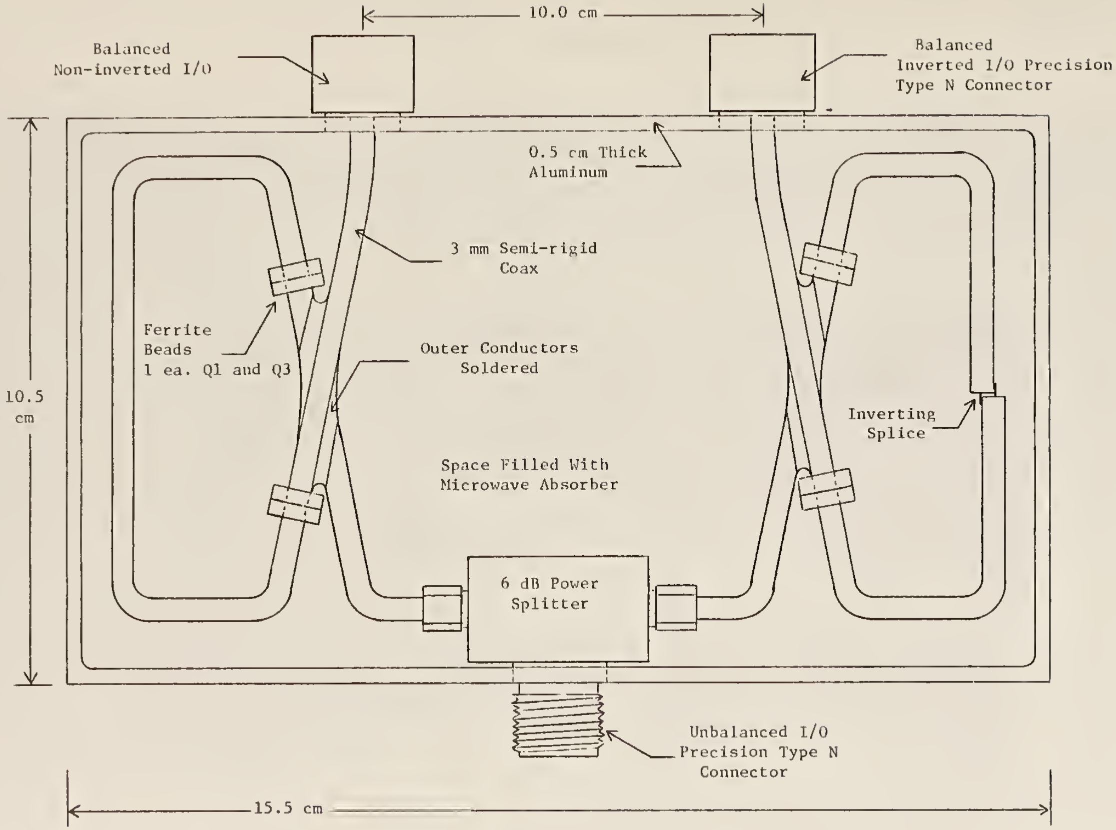

Figure 20. Impulse balun.

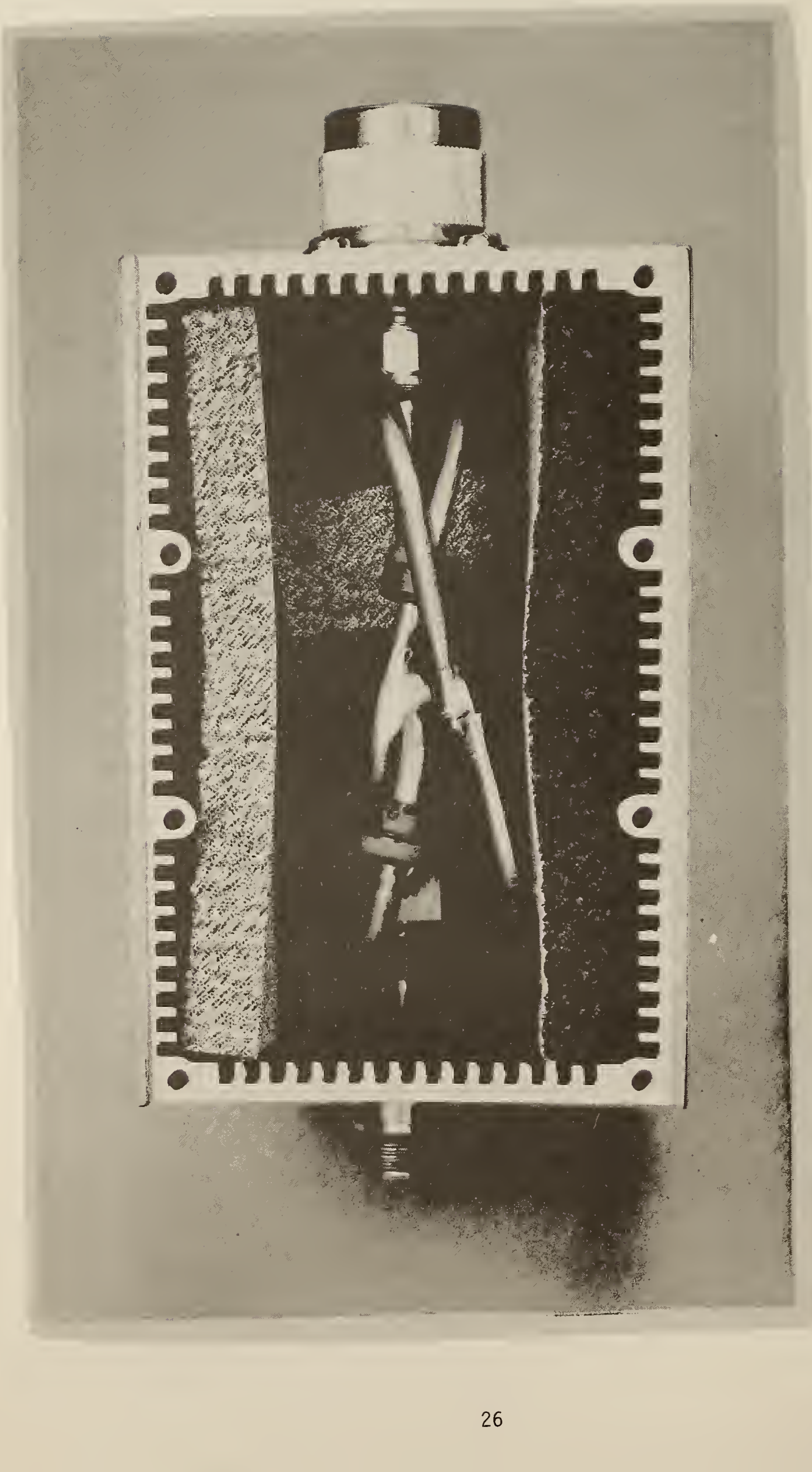

Figure 21. Balun construction.

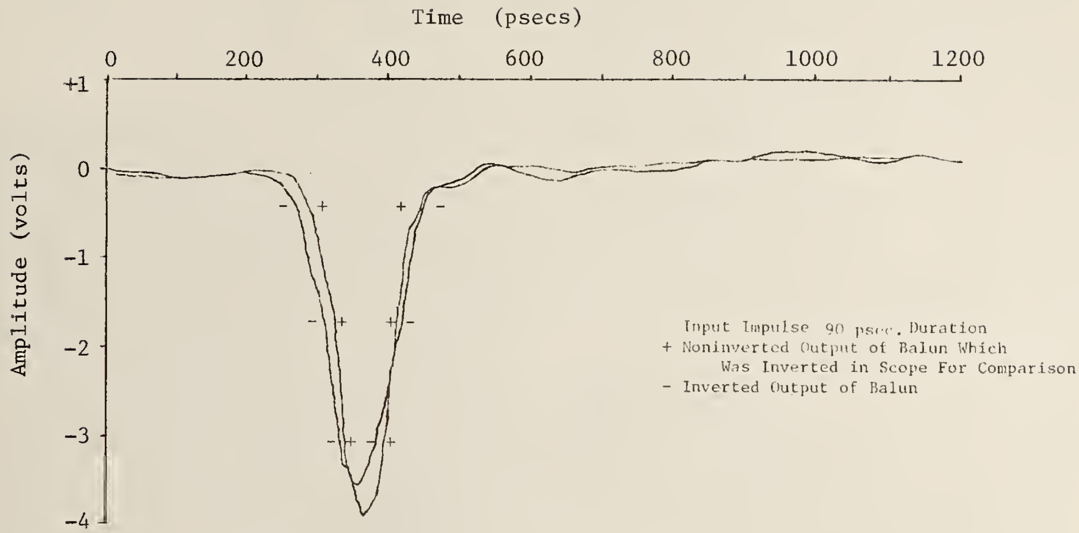

Figure 22. Comparison of the time domain responses of the balun.

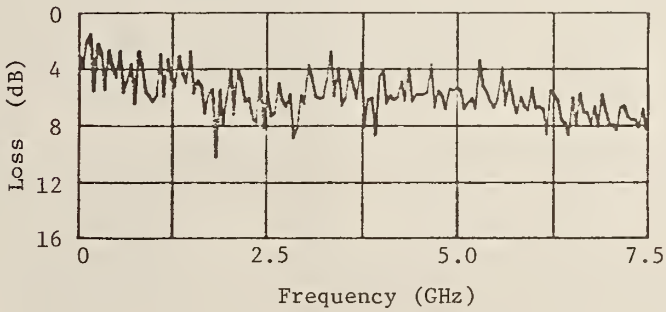

Figure 23. Frequency domain response of baluns.

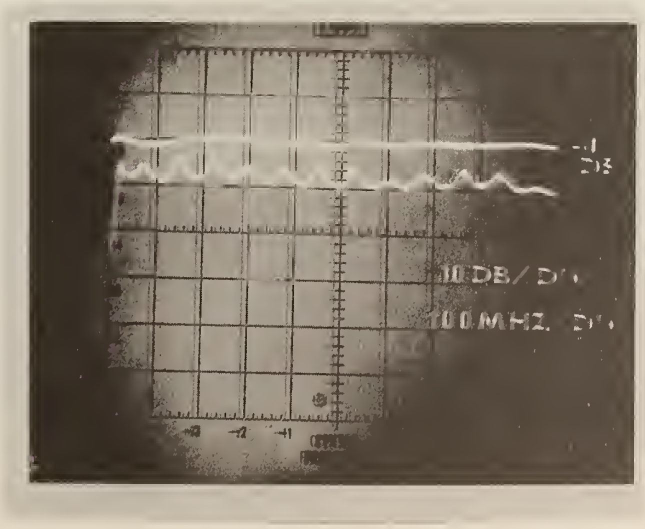

Figure 24. Frequency domain response of baluns using swept frequency techniques.

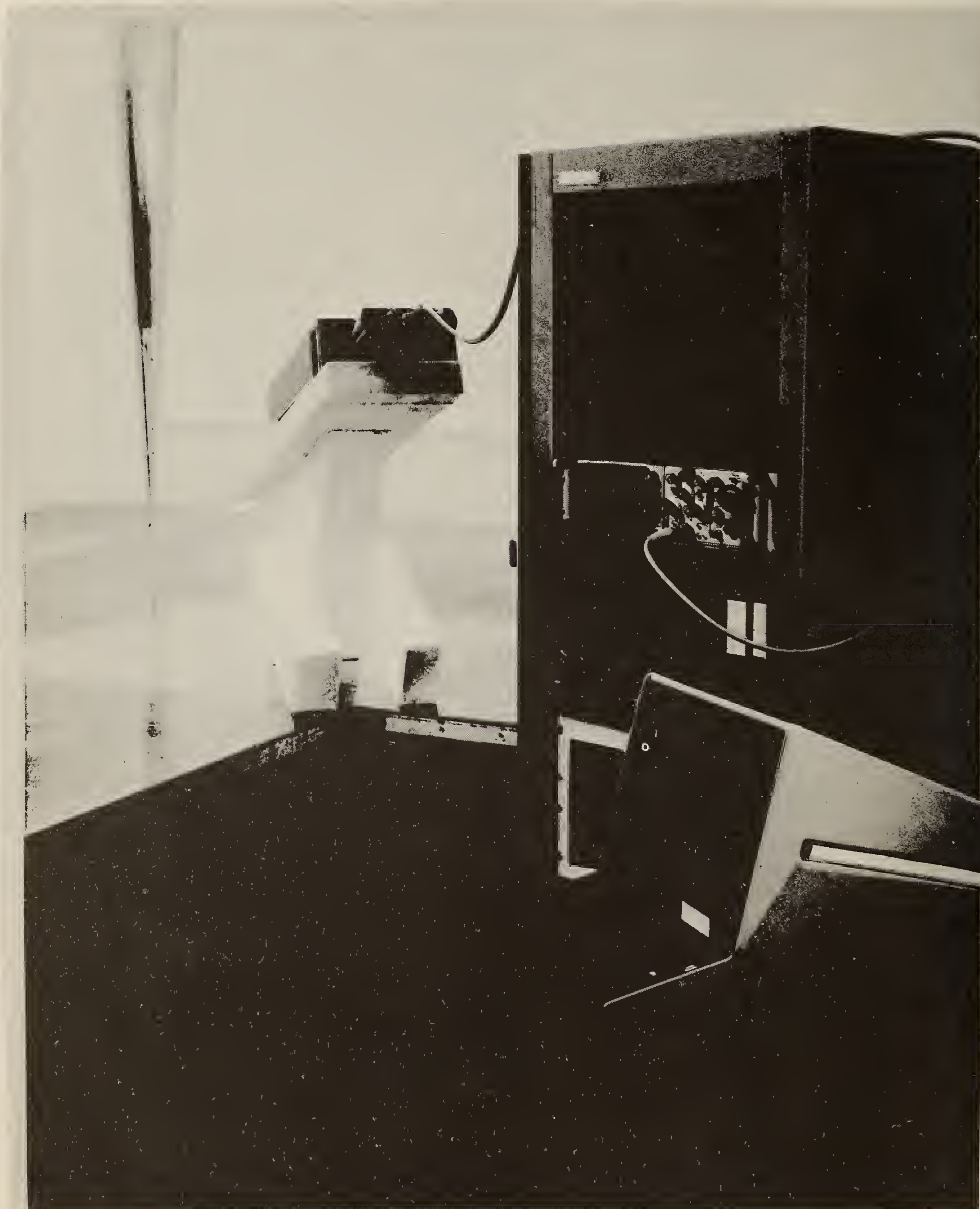

Figure 25. Calibrating a horn over the ground plane.

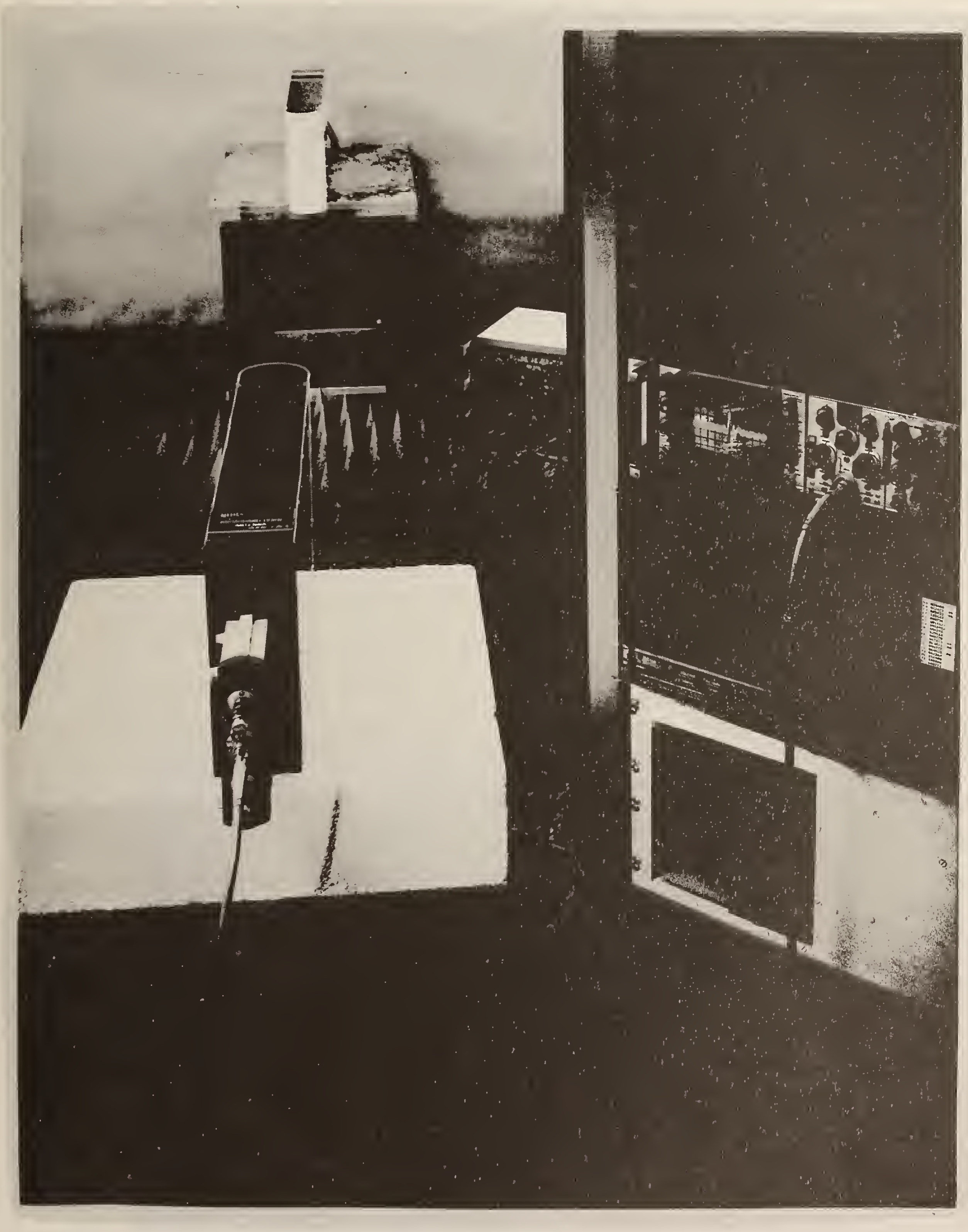

Figure 26. Measurements on the TEM horn.

Figure 27. Resistive monopole on the ground plane.

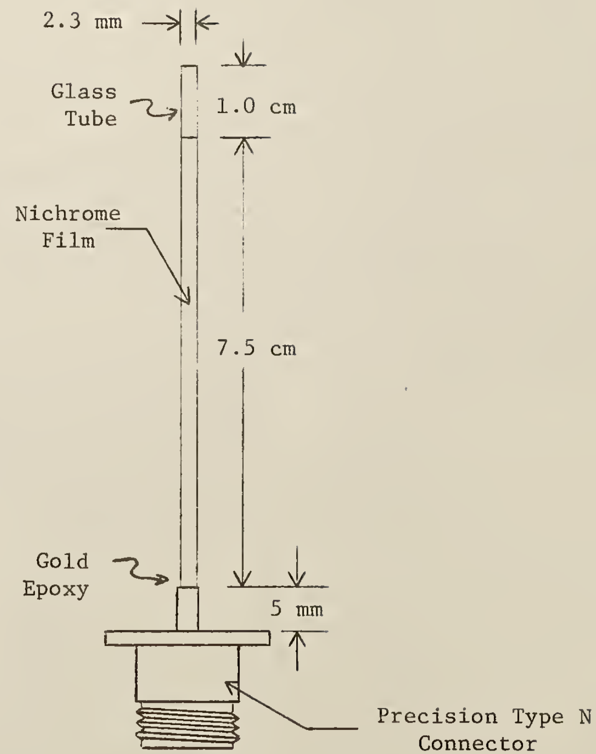

Figure 28. Resistively loaded monopole.

For the two horn measurement, the most serious reflection comes from the floor surface. Since the path length from one horn to the other by way of a single reflection from the floor is three meters (a half meter longer than the direct path), reflections from the floor arrived at the receiver only 1.5 ns after the desired pulse and could interfere with a measurement of the transfer function. The floor was covered with microwave absorber as in the photo which reduced the effect of the reflections.

4.3 Resistively Loaded Monopole

The wave generated by the conical antenna is spherical, and an accurate measurement will be done best if the receiving antenna is small in all dimensions. Considering a dipole (monopole on the ground plane), however, the greatest sensitivity is obtained near the resonant frequency which is a function of its length. Very small dipoles driving a low impedance, say 50 ohms, can be expected to work best at frequencies near resonance and not be particularly broadband. This should not be confused with statements indicating that capacitively loaded miniature dipoles are broadband. Small metal dipoles are broadband if the only load they must drive is a small capacitance. These are useful for measuring cw or peak pulse fields, but this broadband quality disappears when the dipole is resistively loaded by a 50 ohm measuring system. The impedance of such a dipole is capacitive and becomes very high at low frequencies making a poor match to 50 ohms.

A resistive monopole was developed at NBS which is small in size and yet broadband in a 50 ohm measurement system. It is described by Kanda [11] and its use in the conical transmission line is shown schematically in figure 1 and in the photograph of figure 27. It mounts through the ground plane with a type N coaxial connector bolted to the under surface. All connections can be kept under the ground plane.

The monopole is constructed of a 2.3 mm diameter glass tube as shown in figure 28. The lower half centimeter has a gold band for making connection to the center pin of the connector. Gold epoxy works well to make the connection. The next 7.5 cm is vacuum coated with Nichrome in such a way that the resistance nearer to the connector is about 30 ohms per cm. Toward the free end, the resistance increases to about 200 ohms/cm (a higher value would be even better). The tapered resistance was obtained by making the deposition with the low resistance end of the substrate much closer to the metal source than the high resistance end. In its present design, the monopole is too fragile for field use and is limited to laboratory applications.

Figure 29 shows a plot of the transmitted impulse and that received by the resistive probe. The similarity indicates that the probe is a high fidelity receiver, and this is further borne out by the broad response indicated in the frequency domain, figure 30. The response of the probe to a plane E field was obtained numerically by Dr. Kanda and is shown in figure 31 together with the experimental results. The agreement was considered adequate for use as a standard receiver on the ground plane. Other antenna types can now be measured, (1) as a receiver using the cone for a standard transmitter, and (2) as a transmitter using the resistive probe as a receiver. The antenna of principal interest is, of course, the TEM horn.

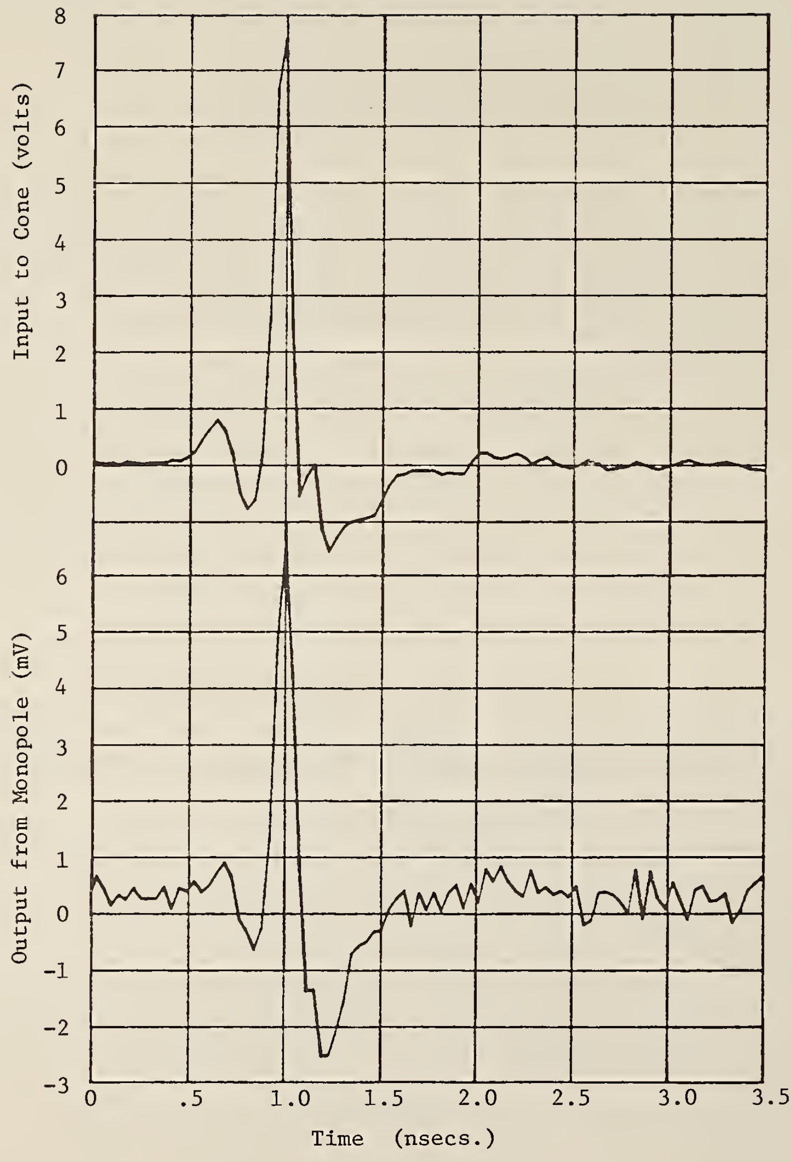

Figure 29. Time domain response of resistive probe.

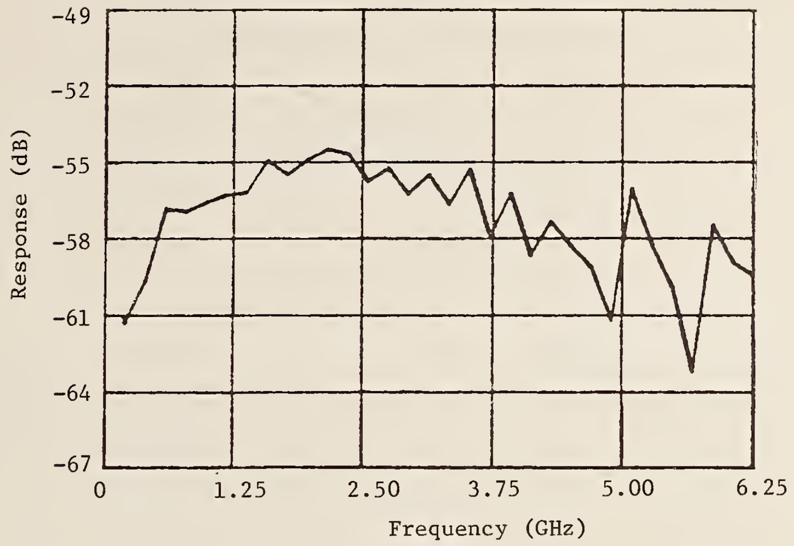

Figure 30. Transfer function of cone-resistive monopole.

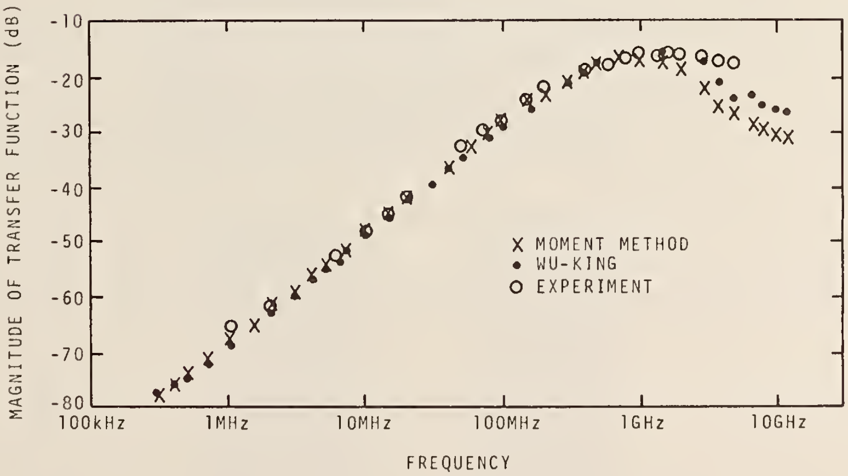

Figure 31. Calculated and measured response of resistively loaded monopole.

5. GENERATORS

As mentioned previously, many different types of signals can be transmitted by a broadband antenna system. To test the impulse response of an antenna pair, the appropriate driving signal is, of course, an impulse. The major part of the work on this project has been done using an impulse generator specifically designed by Dr. James R. Andrews. The design was described at the 1975 IEEE Symposium on EMC and is contained in the proceedings of that symposium (Oct. 1975) [12]. Dr. Andrews has included all the design information in an NBS Report written with M. G. Arthur, titled "Spectrum Amplitude, Definition, Generation and Measurement" [13].

The generator output has already been shown in figure 8. The impulse is approximately 10 volts high and 180 ps wide at its base. The spectrum is shown graphed in figure 32 and tabulated in figure 33, and can be seen to be flat within ± 4 dB from 100 MHz to 4 GHz, and is only 14 dB down at 7 GHz. The generator impedance is nearly 50 ohms due to the back-matching effect of a directional coupler used in the output stage. Since the horns being driven by the generator have a substantial reflection at the radiating aperture, it is necessary to maintain this backmatching to reduce multiple reflections.

To extend the work to higher frequencies, it is possible to amplify the impulse in a Traveling Wave Tube Amplifier (TWTA). The output waveshape no longer resembles an impulse but still has a relatively broad spectrum. Using a C band amplifier, one can generate usable frequency components from below 2 GHz to well above 12 GHz. The output spectrum of an X band amplifier covers 2 - 16 GHz with only one serious resonance at 9 GHz. For more information, see Dr. Andrew's report [13] mentioned previously.

It has also been mentioned that the TEM horn differentiates the driving signal when it radiates. If the measurement calls for a broadband impulsive EM field (for example, to test the impulse response of a receiving antenna alone), it would be better to drive the transmitting horn with a fast rising step function. A long time duration square wave having extremely fast rise and fall times will give equivalent results. Figures 34 and 35 show a square wave and impulsive transmitted wave forms, respectively. The differentiation produces a field composed of a series of impulses having alternating polarity. Experiments have been done with square wave sources with favorable results, and are reported in the next section.

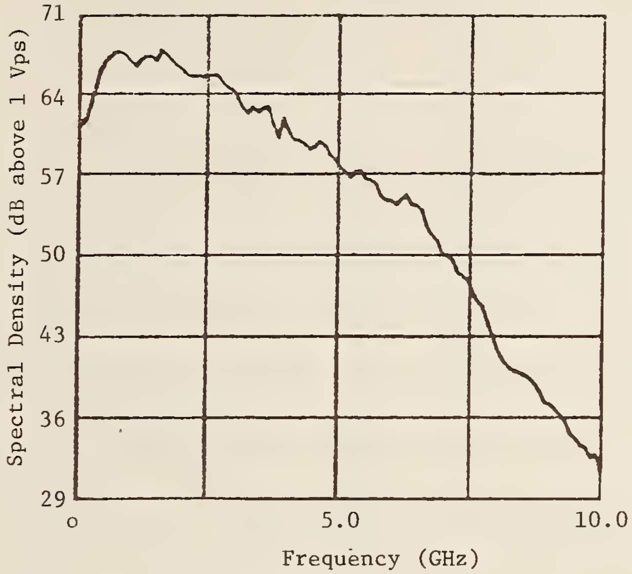

Figure 32. Spectrum of Andrew's impulse generator.

```
SP
*WAVEFORM TYPE? -1=STEP, 0=IMPULSE0
WAVEFORM ACQUISITION MODE? 1=SWEEP SEQUENTIAL,
0=POINT SEQUENTIAL1
NUMBER OF DUMMY DATA ACQUISITION SWEEPS =?30
NUMBER OF WAVEFORM POINTS =?512
NUMBER OF TIME-AVERAGED WAVEFORMS=?100
VERTICAL SCALE FACTOR IN MV/CM=?2000
TIME SCALE FACTOR IN NSEC/CM =?1
INDIVIDUAL SPAMP LISTINGS? (1=YES, 0=NO)1
NUMBER OF FREQUENCY DOMAIN AVERAGES=?1
Y-AXIS CALIBRATION? (1=YES, 0=NO)0
X-AXIS CALIBRATION? (1=YES, 0=NO)0


LISTING UNITS? -1=DB, 0=V-PS -1
     100.000 MHZ          60.212 DB
     200.000 MHZ          60.641 DB
     300.000 MHZ          61.940 DB
     400.000 MHZ          63.511 DB
     500.000 MHZ          65.006 DB
     600.000 MHZ          65.882 DB
     700.000 MHZ          66.288 DB
     800.000 MHZ          66.676 DB
     900.000 MHZ          66.656 DB
    1000.000 MHZ          66.449 DB
    1100.000 MHZ          65.826 DB
    1200.000 MHZ          65.448 DB
    1300.000 MHZ          65.964 DB
    1400.000 MHZ          66.351 DB
    1500.000 MHZ          66.281 DB
    1600.000 MHZ          65.880 DB
    1700.000 MHZ          66.869 DB
    1800.000 MHZ          66.433 DB
    1900.000 MHZ          65.945 DB
```

Figure 33. Spectrum of Andrew's impulse generator.

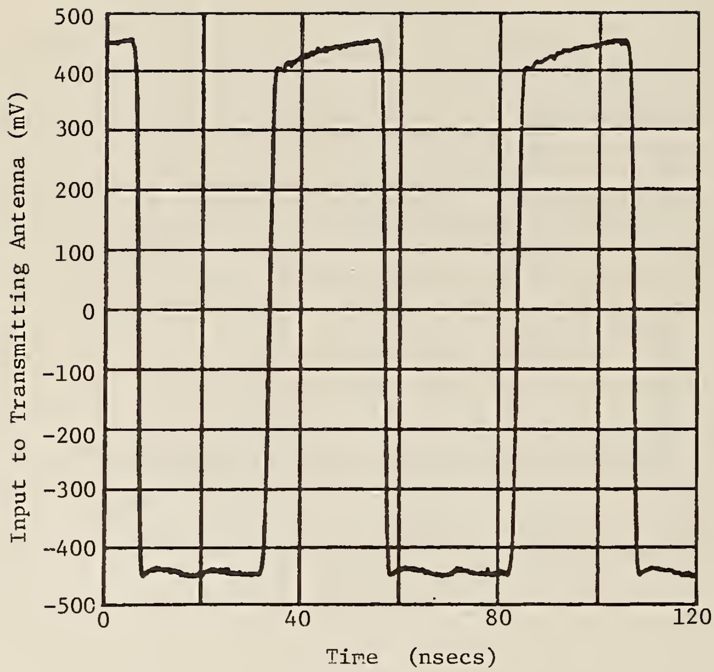

Figure 34. Square wave driving transmitting antenna.

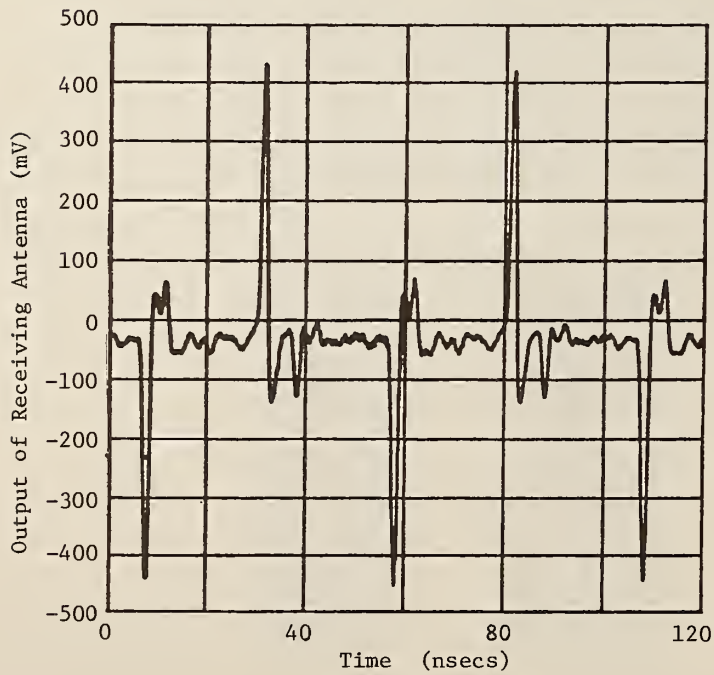

Figure 35. Signal received from a transmitted square wave.

6. MEASUREMENT RESULTS

6.1 Description of Measurements

Before the radiating characteristics of the horn antennas could be measured, the standard cone had to be evaluated. The impedance was measured using the APMS, and the magnitude lies between the limits of 140 and 270 ohms, and errors from this source are discussed in the next section. The 30 cm length of coax-feed line to the cone antenna has a loss which is a function of frequency. This was also measured with the APMS, and the average loss is 0.3 dB with a maximum deviation of ± .3 dB. By assuming that the antenna impedance is a flat 200 ohms and correcting the coax loss at a flat 0.3 dB, an error of approximately ± 1 dB can accumulate.

Now the cone transmit function is calculated for the E field at any point, $P(\theta,r)$, on or above the ground plane. For the layout shown in figures 10 and 25, the distance r is 2.5 meters (adequate for far field). With the horn antenna positioned at 16° above the ground plane, θ will be 74°. For a 200 ohm cone impedance, the voltage on the cone is 1.6 times the incident driving voltage. Therefore, the transmit function can be calculated by substituting into eq. (18) and using eq. (4),

$$T_c(\omega) = \frac{E_\theta(\omega)}{V_{meas}(\omega)} = \frac{1.6}{r \sin(\theta) \ln \left(\cot \frac{\theta_o}{2}\right)} = \frac{1.6}{2.5 (\sin 74.2°) \ln (\cot 2°)} = .2 \frac{V/m}{V} .$$

Measurements made over the ground plane as shown in figure 1, include the combined transfer function of the cone transmitting and horn receiving functions or $T_c R_h$. When this is expressed in dB, the product becomes the complex sum $T_{cdB} + R_{hdB}$ where $T_{cdB} = 20 \text{ Log}_{10} T_c$, R_{hdB} is similarly defined, and these are complex Logarithms. However, our calculations of R_{hdB}, T_{cdB}, and T_{hdB} will only include the magnitude and not the angle. In dB, the cone transfer function becomes -14.1 dB referenced to 1 $\frac{V/m}{V}$. Reducing this by the 0.3 dB coax loss yields

$$T_{cdB} = -14.4 \text{ dB } \frac{V/m}{V} . \tag{20}$$

To calculate the receiving characteristic of the horn alone, we simply subtract the cone function or

$$R_{hdB} = [T_{cdB} + R_{hdB}] - T_{cdB} = [T_{cdB} + R_{hdB}] + 14.4 \text{ dB}.$$

As mentioned in section 2, there is another method for determining the receive function using three horn antennas. Measurements were made using several combinations of the four available horns. Substituting in eq. (9), the values of S_{41} and S_{42} for S_{13} and S_{23}, respectively, (using horn 4 instead of 3)

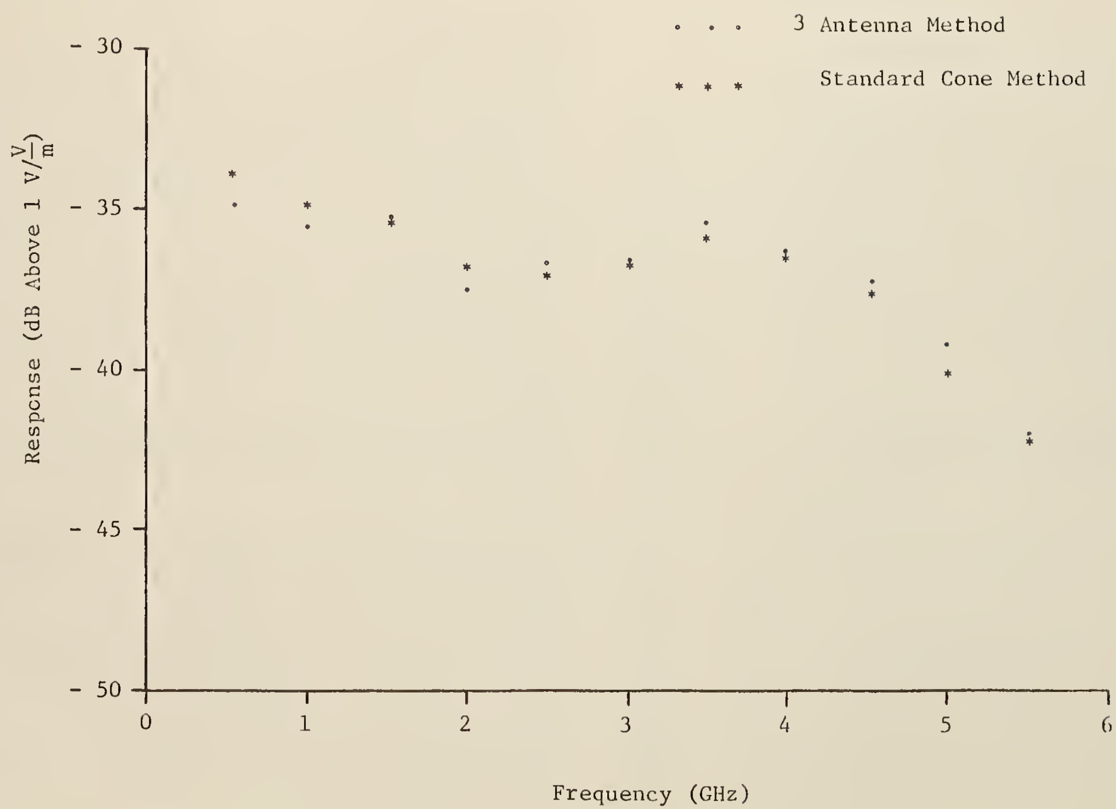

Figure 36. Comparison of different receive functions for horn 1.

$$R'_{h1} = \left(\frac{iZ_o}{\eta} \lambda r_o \frac{S_{41}S_{12}}{S_{42}}\right)^{1/2} e^{\frac{ikr_o}{2}} . \tag{21}$$

The magnitude of this receive function has been calculated and is shown together with the first method for horn 1 in figure 36. The difference is probably due to near-field effects, the cone transmitting function, and reflections, to mention just a few sources. Data determined by these two methods were averaged and are shown for horn 1 and horn 3 in figures 37 and 38, respectively.

Measurements of the transmit function according to the method in eq. (6b) are made by transmitting from one horn antenna and receiving on a similar antenna. The transfer function is again a combination of $T_h R_h$, and expressed in dB, these become $T_{hdB} + R_{hdB}$. To determine the transmit function alone, we simply subtract the horn receiving function determined in the previous experiment or

$$T_{hdB} = [T_{hdB} + R_{hdB}] - R_{hdB}. \tag{22}$$

Now since there are two determinations of the receiving function, R_h measured with the standard cone and R'_h measured by the three antenna method, there can be two different determinations of T_h. This method is really a deconvolution of a receiving function from a combination of transmit and receive functions. Accordingly, the two determinations will be distinguished by calling the first cone deconvolution, and the second three antenna deconvolution.

As mentioned earlier in this report, a second method is also available for determining the transmitting function of the horn antenna. It is shown in section 2, eq. (7), that the transmit and receive functions are related by the following equation,

$$\left|T_h\right| = \left|\frac{\eta R_h}{Z_o \lambda r}\right| .$$

For example, at a frequency of 4 GHz and at the normalizing distance of 1 meter, and a 50 ohm source, $|T_h| = 100.5|R_h|$. In dB, this becomes

$$T_{hdB} = R_{hdB} + 40.0 \text{ dB} \tag{23}$$

In this method the transmit function is determined directly from the receive function and it will be referred to as the direct method.

Results of this determination and the two deconvolution determinations for horn 1 are shown in figure 39 for comparison. Note that the two deconvolution curves agree to about the same degree as the receiving functions do. The direct method data disagrees more, especially at the higher frequencies as expected due to the increasing uncertainty in the standard cone transmit function at those frequencies. The three determinations were averaged for the final data and these are shown for horn 1 and horn 3 in figures 40 and 41, respectively.

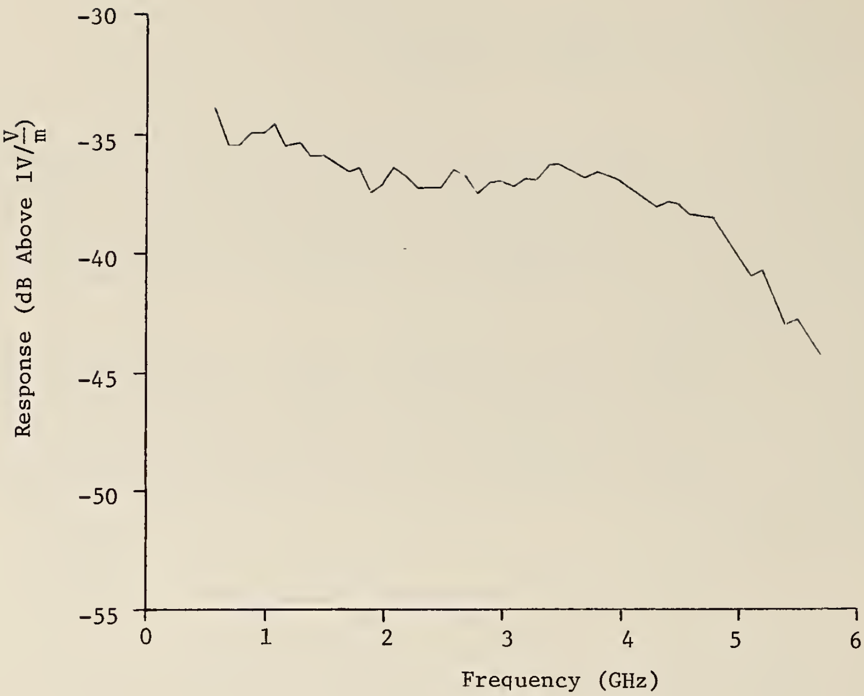

Figure 37. Receiving frequency response of horn 1.

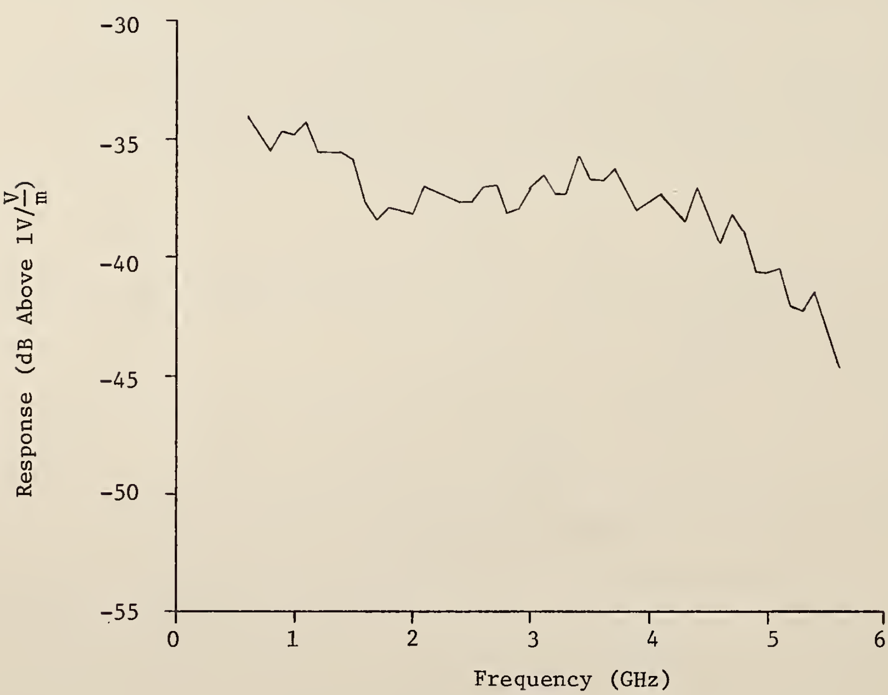

Figure 38. Receiving frequency response of horn 3.

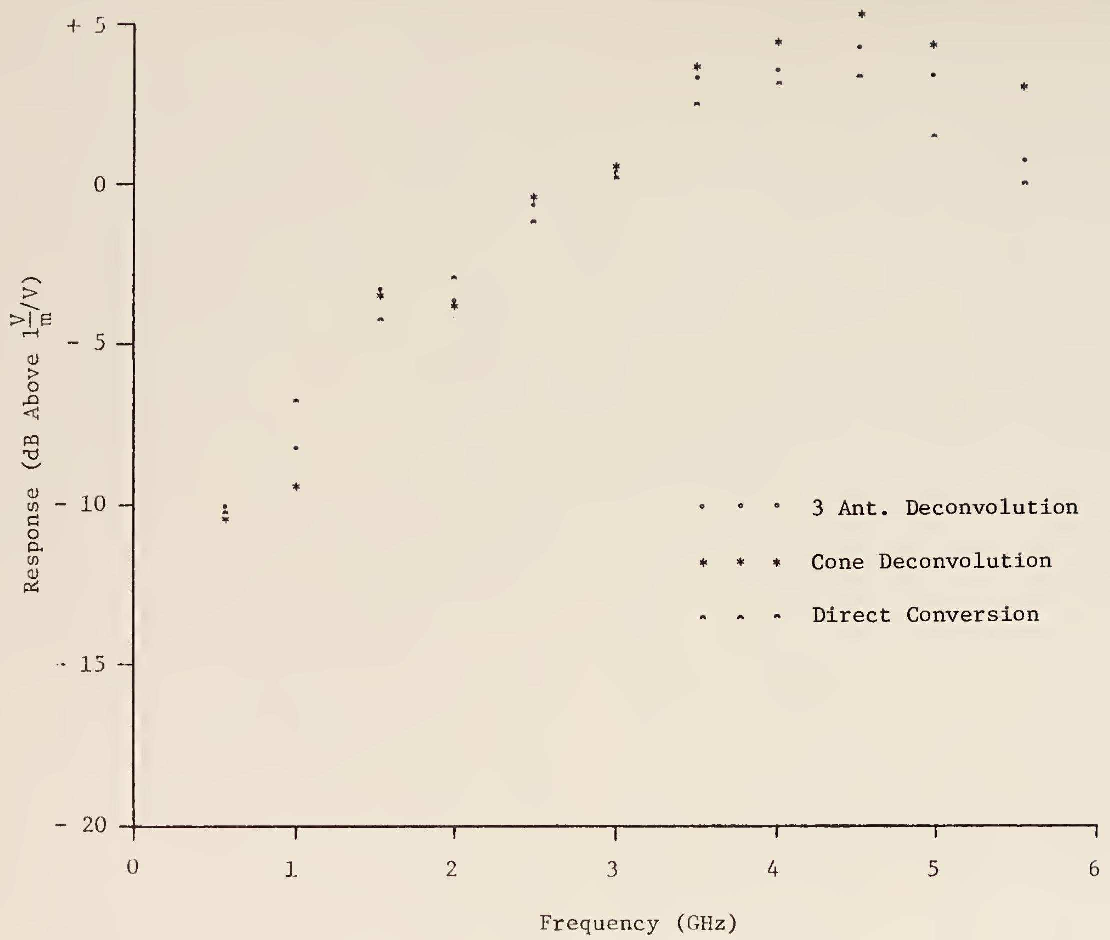

Figure 39. Comparison of different transmit responses for horn 1.

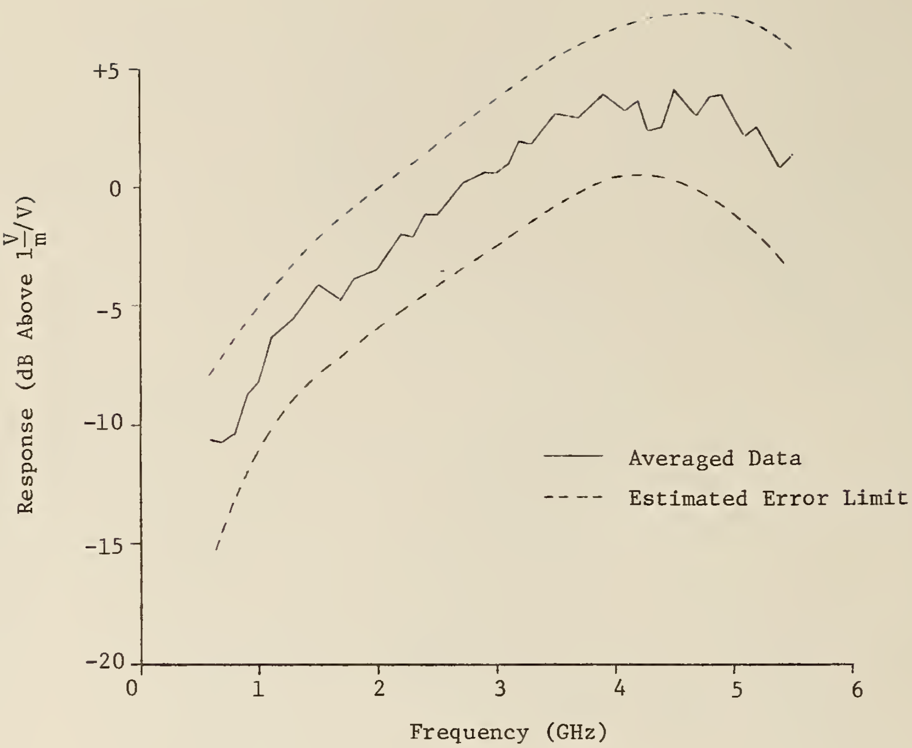

Figure 40. Transmitting frequency response of horn 1.

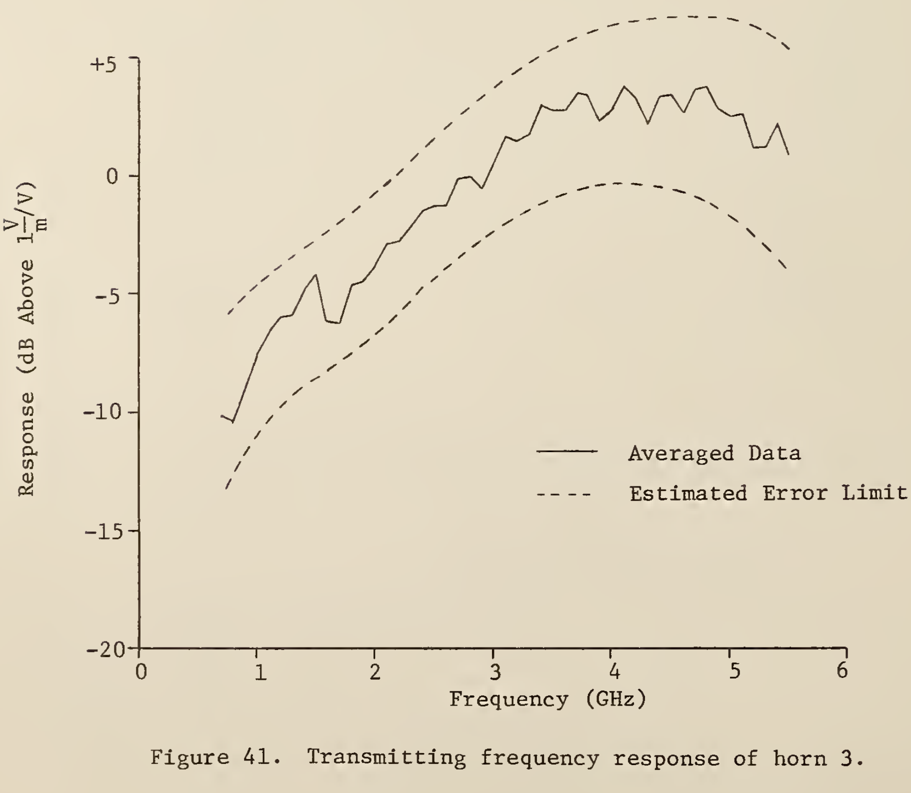

Figure 41. Transmitting frequency response of horn 3.

6.2 Evaluation of Errors

As shown in eqs. (10a) and (10b), there are different sources of error for the two methods of measuring R. This is also true for T. Consider first, the determination of a horn receiving function from measurements with the standard cone. Equation (10a) divides the sources of error into those associated with the cone transmit function, and those produced during the measurement of the cone-horn transfer function S_{hc}.

The cone transmit function is determined theoretically, and is well documented. The one major source of error, as was stated previously, is the impedance of the cone and its input transmission line. These effect the voltage dividing ratio directly, and when multiple reflections between the generator and the base of the cone together with the error in measuring the impedance are included, there is an uncertainty of ± 0.7 dB in the total transmission function.

There is an additional error caused by losses in the input transmission line and these losses together with the uncertainty in their measurement are estimated to be an additional ± .3 dB. A large part of these errors can be measured and calibrated out. This will be done for future work, but for the present time, the entire effect is included as an uncertainty to give a total of ± 1.0 dB. In addition, errors in the measurement of S_{hc} are caused by the limitations of the APMS and have been estimated to be approximately ± 1.0 dB over the frequency range of these measurements [12]. The total uncertainty is ± 2 dB when the antennas are used in a laboratory environment, that is, where both the external (room) reflections and the internal ones due to the balun have been eliminated or time windowed out. This is the way we have normally used them.

When the antennas are used in the field with some type of EMC receiver the balun is necessary and its reflection cannot be time windowed. The reflection occurs in the following way. A signal propagates from the driving point of the antenna and reaches the aperture, where it sees an impedance higher than 50 ohms and is reflected back to the generator. However, as it enters the balun, there is only 6 dB isolation between the two antenna ports, and some of the reflected signal couples to the other side of the antenna and repeats the reflection. Since it requires 12 ns to complete this "reflection cycle" and the maximum duration time window presently obtainable in our facility is only 10 ns, the effect cannot be directly measured. An estimate has been computed from the measured reflection coefficients of both the antenna and balun. The most serious effect is produced at lower frequencies because the antenna is less efficient and its reflection coefficient is higher. Since the error is changing rapidly with frequency, an accurate estimate is very difficult, and for this reason it is not calibrated out. An uncertainty of ± 3 dB is incurred by this effect below 1 GHz and ± 2 dB above 1 GHz. This is then added to the other two errors for a worst case total of ± 5 dB below 1 GHz and ± 4 dB above.

Now, consider the determination of the receiving function by the three antenna method. Equation (10b) shows that the sources of error will be the measurement of the horn transfer

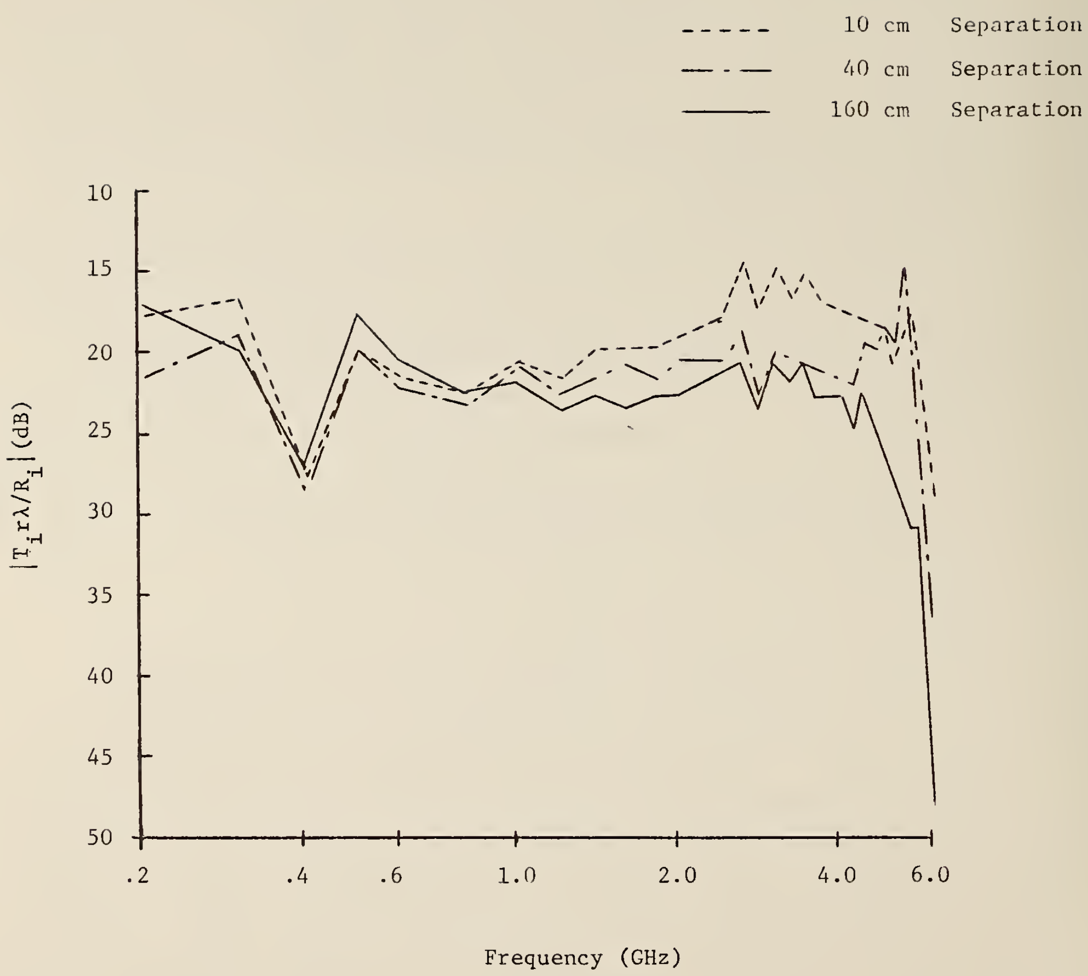

Figure 42. Effect of antenna separation on frequency response.

functions S_{13}, S_{12}, S_{23} and the measurement of the distance r_o. This last factor can be measured accurately and the error considered negligible. Each of the transfer functions have a potential error due to the ± 1 dB uncertainty in the APMS. Equation (10b) shows these three errors and indicates that the S_{23} error subtracts from the other two and this is indeed the case for systematic errors where the measurement system introduces a bias of the same sign to each transfer function. However, the random error in each transfer function does not necessarily have the same sign at all times and on the average does not subtract. Simply adding the three errors together for a worst case combination gives ± 3 dB. This will be the total error under the laboratory conditions discussed above.

For field measurements, the balun reflection error must again be included. The total uncertainty in the measurement increases to ± 6 dB below 1 GHz and ± 5 dB above.

Figure 36 shows that the receiving function of horn 1 determined by these two methods not including the reflection error, has a maximum difference over the frequency range 600 MHz to 5.5 GHz of ± 2 dB, which is within the estimated error bounds of each system individually.

Finally, an error is introduced when the receiving antenna is not in the far field of the transmitting antenna. These effects are estimated by measuring the transfer function of a pair of horns at several spacings (see fig. 42). In changing the spacing of the antennas, the pattern of reflections from the walls and floor also changes, so that not all the variations in transfer function can be attributed to near-field effects. However, since the data taken with a 10 cm spacing between antennas diverges from the 40 cm and 160 cm data above 2 GHz, it can be safely said that the near-field effects over the frequency range of 600 MHz to 5 GHz exceed ± 3 dB when the spacing is reduced to less than 40 cm. The larger error occurs at the higher frequencies where the near-field region extends farther in front of the antenna than at lower frequencies. At distances of 2.5 meters, at which our measurements were made, the near-field effect should be small (at worst .1 dB for cone transmitter).

The transmit functions for the horns determined in the two ways each have their own particular sources of error. In the first case, the uncertainty in $[T_{hdB} + R_{hdB}]$ is given by the uncertainty in S_{hh}. The uncertainty in R_{hdB} is described above. The total uncertainty for this determination is estimated to be the sum of the two or ± 3 dB over the frequency range.

A third determination of the transmit function is calculated from the receive function according to Kerns [16] and has exactly the same uncertainty as that function. Therefore, the estimated uncertainty at worst is again given as ± 3 dB over the frequency range. In both cases, however, if balun reflection errors must be included, then the total worst case uncertainty increases to ± 6 dB below 1 GHz and ± 5 dB above 1 GHz.

Notice that the measured value of the received function appears in eq. (23) with a positive sign, while in eq. (22) the sign is negative. It should be expected then, that any systematic errors in measuring R_h will have the opposite effect in the two determinations of T_h. The three curves shown in figure 39 agree well in the range of 600 MHz to 2 GHz, to within 2 dB up to 4 GHz, and no worse than 3 dB to 5.5 GHz. The increasing difference is attributed partly to the small near-field effects which become more pronounced at high frequencies, and partly due to errors in the cone transmitting function. Notice that the determination based on the three antenna receive function lies between the other two curves. The fact that the three antenna method does not require the standard cone indicates that this difference is probably due to the cone. These results verify the measurement technique and give an estimate of the error.

7. RECOMMENDED USE OF ANTENNAS FOR FIELD GENERATION

The horn antennas were designed to permit the user to establish a known impulsive field on his own antenna range. The horn selected as transmitter is positioned on the range between 2 and 3 meters from the device being evaluated (usually an unknown antenna). The antenna is driven from a well-matched 50 ohm waveform generator, either impulse-like or sinusoidal, through some length of 50 ohm coaxial transmission line. The spectral intensity (or output voltage for sinusoidal generators) must be known for the generator and cable into a 50 ohm load.

The unknown device being evaluated is temporarily replaced by a second horn connected to a precision receiver by a length of 50 ohm coaxial cable and this receiver must also present a good 50 ohm termination to the cable. Certain spectrum analyzers and precision receivers present a better match than others and this should be a major consideration in selecting one.

Now, the field at the receiving site can be calculated from the known waveform generator spectrum and the transmitting function of the horn. But it can also be measured by the standard receiving system and the values determined by each method should correlate. Differences greater than a few dB usually indicate spurious reflections on the range.

To determine the field intensity at any distance along the antenna boresight when the generator produces a sinusoidal voltage, simply multiply the generator output voltage into a 50 ohm load by the transmit transfer function and divide by D, the ratio of the distance in meters r to a reference distance of 1 meter, or

$$E = VT_h/D.$$

Note that D is dimensionless and T_h has dimensions of volts per meter/volt. This is valid only for those values of D that ensure far-field conditions. When this is expressed in dB, as in appendix B, simply add the generator voltage in dB above 1 volt and subtract the distance ratio in dB from the transfer function in dB giving the field strength in dB above 1 volt/meter,

$$E_{dBV/m} = V_{dBV} + T_{hdB/m} - D_{dB} .$$

The same equation is used when the input is an impulse, and its spectrum (S_{dB}) is given in dB above 1 volt-picosecond as is the case for Andrews' impulse generator. We define spectrum of the field (E'_{dB}) as

$$E'_{dBVps/m} = S_{dBVps} + T_{hdB/m} - D_{dB} , \tag{24}$$

where $E'_{dBVps/m}$ has dimensions of dB above 1 volt-picosecond per meter, and S_{dBVps} is the spectral intensity of the impulse generator in dB above 1 volt-picosecond.

If the spectrum of the input waveform is given in microvolts per megahertz (μV/MHz), the numbers will be exactly the same as above since

$$1\ \mu V/MHz = 1\ V\text{-}ps ,$$

and the field spectrum will be given in dB above 1 μV/MHz per meter. For example, figure 33 shows that the Andrews' impulse generator has a spectrum of 66.4 dB above 1 V-ps in the vicinity of 1 GHz. Using horn 1 to transmit, Appendix B shows its response at 1 GHz to be -8.1 dB $\frac{V/m}{V}$ at a distance of 1 m. At 40 cm separation, the signal would increase by a factor of 2.5 or 8.0 dB. The field spectrum from horn 1 at 40 cm would then be

$$E'_{dB} = 66.4\ dB + (-8.1\ dB) - (-8.0\ dB) = 66.3\ dB\ \frac{V\text{-}ps}{m} .$$

The receiving characteristics can be used to check this field spectrum value. Suppose horn 3 was located 40 cm from horn 1 which was transmitting the signal described above. The voltage that horn 3 should supply to a 50 ohm receiver is simply the electric field times the receive transfer function

$$V_R = E\ R_H ,$$

or in dB

$$V_{RdB} = E_{dB} + R_{HdB} .$$

Since the receiving function is measured with respect to the field at the receiving antenna aperture, there is no distance adjustment. For a broadband signal, the equation gives the spectrum of the received voltage waveforms (S_{RdB}) as

$$S_{RdB} = E'_{dB} + R_{HdB} . \tag{25}$$

Appendix B shows the receive function of horn 3 at 1 GHz to be -35.0 dB with respect to 1 $V/\frac{V}{m}$ and so the received spectrum should be

$$S_{RdB} = +\ 66.4\ dB - 35.0\ dB = 31.4\ dB\ V\text{-}ps$$

This can be measured using a spectrum analyzer as a receiver. The results of this measurement yielded 28 dB on a 1 MHz bandwidth when the proper corrections were applied.

$$S_{RdB} = S_{mdB} - BW_{dB} + 107 \text{ dB} + 3 \text{ dB}$$

$$= - 79 \text{ dB} - 3 \text{ dB} + 107 \text{ dB} + 3 \text{ dB}$$

$$= + 28 \text{ dB } \mu\text{V/MHz}$$

where

S_{mdB} is the measured spectrum in dBm

BW_{dB} is the ratio of actual bandwidth to 1 MHz

107 dB is used to convert dBm to dBμV

3 dB is added to convert RMS to peak volts.

The same spectrum measured on the APMS resulted in a figure of 30.5 dBμV/MHz and on a commercial EMI receiver using only handbook calibrations, 28 dBμV/MHz.

It is interesting though that the signal is only 4 dB above the noise in the EMI receiver having a bandwidth of 500 kHz; 10 dB above the noise for the spectrum analyzer with 1 MHz bandwidth, or 20 dB for 3 MHz. The APMS was still making valid measurements 40 dB below this level and extended to 50 dB when the integration time was increased to 1 minute (the repetition rate for the impulse generator was 50 kHz for all measurements). This minimum equivalent input to the APMS was -20 dBμV/MHz or 0.1 μV/MHz. The increased sensitivity is due to the signal processing that the APMS can do when it has the prior knowledge of when the signal will occur.

The received signal strength diminishes rapidly as the antennas are separated, and the signal will be lost in the noise at a 1 meter spacing if the EMI receiver is used. The spectrum analyzer, when used on the 3 MHz bandwidth will give the same results with the antenna spacing increased to 3 meters. The superior bandwidth of the APMS allowed excellent measurements to be taken at 3 meter spacing and should still operate well at over 100 meters if reflections could be controlled.

In view of the results obtained in the near-field measurement, it is recommended that the horn antenna pair be used with spacings between one meter and three meters. For a horn transmitter and some other receiving antenna, the spacing may have to be increased because of the possible near-field effects due to the receiver antenna.

8. CONCLUSIONS

A method for measuring antenna transfer functions in the time domain was developed, and the technology is now available to measure the transmitting and receiving functions of most antennas. Given this capability, the receiving characteristic of a variety of antenna types was measured, and the TEM horn was selected as the most promising candidate for a transfer standard antenna.

TEM horn characteristics were measured on a ground plane and in a free-space field environment. Preliminary measurements indicate that the receiving characteristics are constant within ± 10 dB from below 100 MHz to above 6 GHz but have only been measured accurately (± 3 dB) between 600 Mhz and 5.5 GHz.

Transmission characteristics were shown to include a 6 dB per octave frequency dependence in accordance with accepted reciprocity relations. This limits the useful transmitting range using impulse excitation to 600 MHz - 5 GHz with a variation from flatness of less than ± 10 dB. However, a flat transmitted field spectrum was obtained when the driving signal was a square wave. Using this signal source, the generated impulsive fields have a reasonably flat spectrum even below 100 MHz.

The limits of error have been estimated to be less than ± 3 dB in the frequency range 600 MHz to 5 GHz as long as the antenna spacing is approximately that of the measurements reported herein, 2.5 meters. The effects of changes in spacing included those due to reflections and near field and did not exceed ± 3 dB over the range 40 cm to 320 cm. Care has to be taken to minimize the effect of reflections from the ground surface and large reflecting surfaces close to the antennas. Using baluns with these antennas added an additional uncertainty of ± 3 dB below 1 GHz and ± 2 dB above 1 GHz.

Feasibility tests have been made with balanced (push-pull output) generators and resistively loaded horns which indicate that much flatter responses and significantly smaller errors can be obtained over a wider frequency range (perhaps ± 3 dB over 100 MHz to 6 GHz).

The preliminary experiments just mentioned indicate that we have good understanding of those factors which must be changed in the TEM horn to extend its frequency both downward to 20 MHz and upwards to at least 8 GHz. The flatness can be significantly improved over this range and, therefore, the sources of errors can be better controlled.

Time did not permit the completion of the Singularity Expansion Method (SEM) and homomorphic analysis mentioned previously, which would be needed to extend the frequency range of the ground plane downward, but even without SEM and with some modifications to the ground plane, it can be used down to 50 MHz. SEM type analysis is expected to extend that downward to 20 MHz and perhaps lower.

The lower frequency work will probably require removing the measurements to the outdoor antenna range which will reduce reflections and allow greater antenna spacing. This had to be postponed for later work, lacking the necessary modifications to the APMS to protect it from the outdoor environment. This is still an important improvement to consider for future work.

APPENDIX A

In this appendix the functional relation between the TEM horn transmitting function, T_H, and receiving function R_H will be derived. As has been noted previously [4,5], these functions are not identical functions of time (frequency). What is the same at a given frequency and to which the usual reciprocity relations refer is directivity or antenna patterns.

Martíns and Van Meter [5] have given a qualitative relation between the electric field generated by a horn and its input voltage, the former being the derivative of the latter, but impedance details are suppressed in their analysis which prohibits one from making a quantitative evaluation.

To obtain the desired result, we will start with a specific example, a uniform sphere and calculate the on axis transmitting function, $T(\omega,r)$, and receiving function, $R(\omega)$. This will then be compared to results we will obtain from equations applicable to an arbitrary antenna. Readers who are interested only in the general result, can proceed directly to the analysis that begins after eq. (A27).

The magnetic field radiated by a gap fed perfectly conducting sphere [6], as shown in figure 43, is

$$H_\phi(\omega,r) = -i\,\frac{\omega\varepsilon a^{\frac{1}{2}}V_o}{r^{\frac{1}{2}}}\sum_{n=1}^{\infty}\frac{(2n+1)P_n^1(o)P_n^1(\cos\theta)}{2n(n+1)}\;\frac{H^{(2)}_{n+\frac{1}{2}}(kr)}{kaH^{(2)}_{n-\frac{1}{2}}(ka)-nH^{(2)}_{n+\frac{1}{2}}(ka)} \tag{A1}$$

where

ε = The medium permittivity

r = the distance from the center of the sphere to the point of observation

a = the radius of the sphere

$k = 2\pi/_\lambda$

V_o = the voltage at the gap

$P_n^1(\cos\theta)$ = the associated Legendre function of the first kind

$H_n^{(2)}(ka)$ = the Hankel function of the second kind which kind is a result of an assumed, but suppressed, time dependence of the field of $e^{+i\omega t}$. This results in a traveling wave in the +r direction.

The transverse component of the electric field, $E_\theta(r,\omega,\theta)$, in the far field can be obtained from eq. (A1) by the usual relation,

$$E_\theta(r,\omega,\theta) = \eta H_\theta(r,\omega,\theta). \tag{A2}$$

The radial function of eq. (A1) in the far field kr>>1, becomes [14]

$$\frac{H^{(2)}_{n+\frac{1}{2}}(kr)}{r^{\frac{1}{2}}} = \sqrt{\frac{2k}{\pi}}\,\frac{1}{kr}\,i^{n-1}\,e^{-ikr}\;. \tag{A3}$$

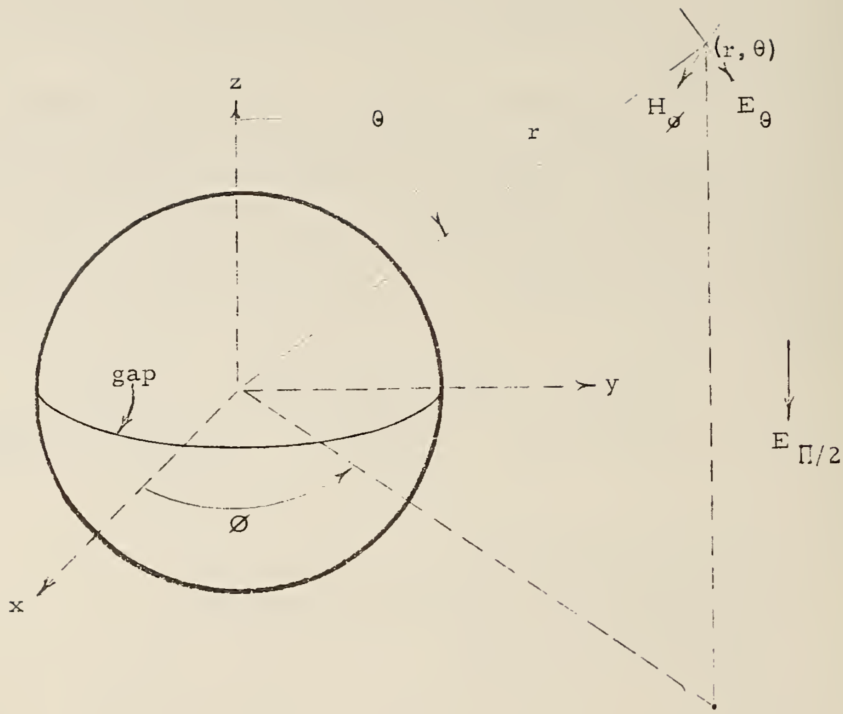

Figure 43. Magnetic field radiated by a conducting sphere.

Also, on axis $P^1(\cos\theta)$ becomes $P_n^1(o)$ which, together with eq. (A3) in eq. (A1) and with the result in eq. (A2), one has

$$E(\omega,r,\tfrac{\pi}{2}) = \frac{\eta V_o}{2}\,\omega\varepsilon a^{1/2}\sqrt{\frac{2k}{\pi}}\,\frac{e^{-ikr}}{kr} \times \sum_{n=1}^{\infty} \frac{i^n(2n+1)}{n(n+1)}\,\frac{[P_n^1(0)]^2}{[kaH_{n-\frac{1}{2}}^{(2)}(ka) - nH_{n+\frac{1}{2}}^{(2)}(ka)]} . \tag{A4}$$

The quantity, $P_n^1(o)$, is given on page 554 of [2] as

$$P_n^1(o) = \frac{(-1)^{-(\frac{n-1}{2})}\,n!}{2^{n-1}[(\frac{n-1}{2})!]^2} \quad \text{for n odd, and} \tag{A5}$$

$$= 0 \quad \text{for n even.}$$

Now for the inverse problem, consider figure 44 which represents a solid metal sphere embedded in a plane wave field with the polarization and propagation directions indicated by the $\overline{E}$ and $\overline{k}$ vectors, respectively. We will solve for the resultant current across the equator at $\phi = \pm\frac{\pi}{2}$. This will be the desired load current, and it will be assumed to be the same as the current, I, that would flow in a real, thin, circular load resistor placed at this equator as long as the conductance, G_L, across this resistor (in the ϕ direction) is much greater than the spherical antenna source admittance (a typical value is .004 ohms for ka = 0.5 [6]).

The voltage, V_L, developed across this conductance then will be

$$V_L = \frac{I}{G_L} . \tag{A6}$$

If we let $\hat{a}_r$ and $\hat{a}_\theta$ represent unit vectors in the r and θ directions, respectively, then the current density, $\overline{J}(\theta)$, at the equator is

$$\overline{J}(\theta) = \hat{a}_r \times \overline{H}(a,\theta,\phi) \tag{A7}$$

and the total current, I_L, is obtained by integrating along the equator or

$$I_L = a\int_o^{\pi} \overline{J}(\theta)\cdot\hat{a}_\phi d\theta\Big|_{\phi=+\frac{\pi}{2}} + a\int_{\pi}^{o} \overline{J}(\theta)\cdot\hat{a}_\phi d(-\theta)\Big|_{\phi=-\frac{\pi}{2}}$$
$$= a\int_o^{\pi} [H(a,\theta,\tfrac{\pi}{2}) + H(a,\theta,-\tfrac{\pi}{2})]d\theta . \tag{A8}$$

The required expression for $H(a,\theta,\phi)$ can be obtained from Stratton [15]. For the problem of interest, the vector function $\overline{m}_{eln}^{(1)}$ will have only a θ component since $\cos(\pm\pi) = 0$. The vector function $n_{oln}^{(1)}$ will not exist since $\cos(\pm\frac{\pi}{2}) = 0$ eliminates the ϕ
$\partial P^1(\cos\theta)$

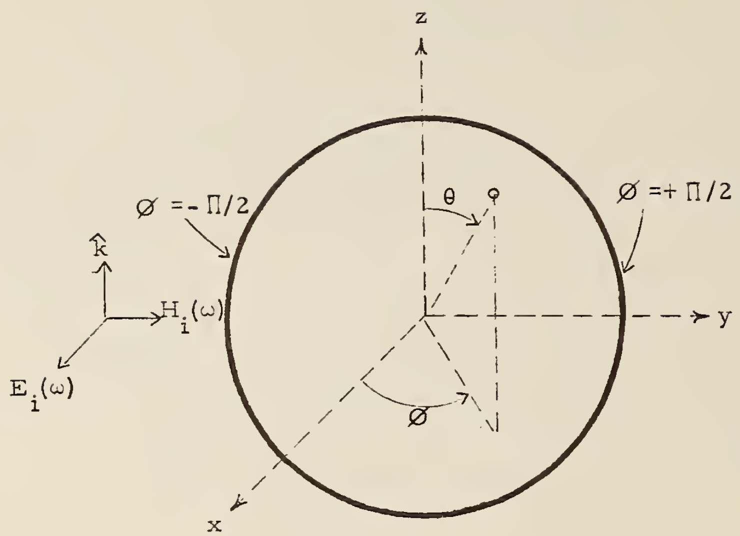

Figure 44. Conducting spherical receiver in a plane wave field.

component, integration of the function, $\frac{n}{\partial\theta}$, over all θ eliminates the θ component, and continuity of the magnetic field at a perfectly conducting boundary requires that the r component be zero.

The explicit result for the sum of the incident, H_{ir}, and reflected, H_{rr}, radial components of the magnetic field is [15]

$$
\begin{aligned}
H_{ir} + H_{rr} &= f(\omega,\theta,\phi)[\overline{n}^{(1)}_{oln} + a^r_n \overline{n}^{(3)}_{oln}] \cdot \hat{a}_r \\
&= f'(\omega,\theta,\phi)[j_n(\rho_o) - \frac{j_n(\rho_o)h_n(\rho_o)}{h_n(\rho_o)}] \qquad \text{(A9)} \\
&= 0,
\end{aligned}
$$

where $\rho_o = ka$, $f(\omega,\theta,\phi)$ and $f'(\omega,\theta,\phi)$ are arbitrary functions independent of r, and $j_n(\rho)$ and $h_n(\rho)$ are spherical Bessel and Hankel functions related to the more conventional functions by

$$j_n(\rho) = \sqrt{\frac{\pi}{2k\rho}}\, J_{n+\frac{1}{2}}(\rho) \qquad \text{(A10)}$$

and

$$h_n^{(1)}(\rho) = \sqrt{\frac{\pi}{2k\rho}}\, H^{(1)}_{n+\frac{1}{2}}(\rho). \qquad \text{(A11)}$$

We are thus left with a single θ component for $m^{(1)}_{eln}$ which yields for the magnetic field

$$\overline{H}_i = \frac{kE_o}{\mu\omega} \sum_{n=1}^{\infty} \frac{i^n(2n+1)}{n(n+1)} \frac{P^1_n(\cos\theta)}{\sin\theta} \sin\theta\, j_n(\rho_o)\hat{a}_\theta \qquad \text{(A12)}$$

where the assumed time dependence, $e^{-i\omega t}$, has been suppressed. Now for the total field

$$
\begin{aligned}
\overline{H}_i + \overline{H}_r &= \frac{kE_o}{\mu\omega} \sum_{n=1}^{\infty} \frac{i^n(2n+1)}{n(n+1)} (\overline{m}^{(1)}_{eln} + b^r_n \overline{m}^{(3)}_{eln}) \\
&= \frac{kE_o}{\mu\omega} \sum_{n=1}^{\infty} \frac{i^n(2n+1)}{n(n+1)} \left[\frac{P^1_n(\cos\theta)}{\sin\theta} \left\{j_n(\rho) - \frac{[\rho j_n(\rho)]'}{[\rho h^{(1)}_n(\rho)]'}\right\}_{\rho=\rho_0}\right] \hat{a}_\theta .
\end{aligned} \qquad \text{(A13)}
$$

where the primes denote differentiation with respect to ρ. In particular,

$$[\rho j_n(\rho)]' = j_n(\rho) + \rho \frac{d}{d\rho} [j_n(\rho)] \qquad \text{(A14)}$$

and

$$[\rho h^{(1)}_n(\rho)]' = h^{(1)}_n(\rho) + \rho\frac{d}{d\rho} [h_n(\rho)]. \qquad \text{(A15)}$$

Therefore, the quantity in the braces becomes

$$\left\{\frac{j_n(\rho)\, h_n^{(1)}(\rho) + \rho j_n(\rho)\frac{d}{d\rho}\,[h_n^{(1)}(\rho)] - j_n(\rho)h_n^{(1)}(\rho) - \rho h_n^{(1)}(\rho)\frac{d}{d\rho}\,[j_n(\rho)]}{h_n^{(1)}(\rho) + \rho\,\frac{d}{d\rho}\,[h_n^{(1)}(\rho)]}\right\}_{\rho=\rho_0} \tag{A16}$$

$$= \rho_o\,\frac{j_n(\rho)\frac{d}{d\rho}\,[h_n^{(1)}(\rho)] - h_n^{(1)}(\rho)\frac{d}{d\rho}\,[j_n(\rho)]}{h_n^{(1)}(\rho) + \rho\,\frac{d}{d\rho}\,[h_n^{(1)}(\rho)]}\Bigg|_{\rho=\rho_0} .$$

Now the quantity in the numerator is simply the Wronskian of $j_n(\rho)$ and $y_n(\rho)$ times i or $i[\frac{1}{\rho^2}]$. To demonstrate this we will substitute

$$h_n^{(1)}(\rho) = j_n(\rho) + iy_n(\rho)$$

in the expression of interest, eq. (A16), which gives [14]

$$j_n(\rho)\left\{\frac{d}{d\rho}\,[j_n(\rho)] + i\,\frac{d}{d\rho}\,[y_n(\rho)]\right\} - \frac{d}{d\rho}\,[j_n(\rho)]\left\{j_n(\rho) + iy_n(\rho)\right\}$$

$$= i\left\{j_n(\rho)\,\frac{d}{d\rho}\,[y_n(\rho)] - y_n(\rho)\,\frac{d}{d\rho}\,[j_n(\rho)]\right\} \tag{A17}$$

$$= i[\frac{1}{\rho^2}].$$

The denominator of eq. (A16) can be expressed in an alternate form by using the recurrence relation [14]

$$\frac{n+1}{\rho}\,h_n^{(1)}(\rho) + \frac{d}{d\rho}\,[h_n^{(1)}(\rho)] = h_{n-1}^{(1)}(\rho) \tag{A18}$$

which together with eq. (A17) in the expression of interest, eq. (A16), gives

$$\rho_o\,\frac{i/\rho_o^2}{\rho_o h_{n-1}^{(1)}(\rho_o) - nh_n^{(1)}(\rho_o)} \tag{A19}$$

for the term in curly brackets, which inserted in eq. (A13) and with that result in eq. (A8) one obtains for the current

$$I = \frac{E_o}{\mu\omega}\,\frac{i\sqrt{2ka}}{\pi}\sum_{n=1}^{\infty}\frac{i^n(2n+1)}{n(n+1)}\;\frac{2\int_o^\pi \frac{P_n^1(\cos\,\theta)}{\sin\,\theta}\,d\theta}{[kaH_{n-\frac{1}{2}}^{(1)}(ka) - nH_{n+\frac{1}{2}}^{(1)}(ka)]} . \tag{A20}$$

Note: If a wave of time dependence, $e^{+i\omega t}$, had been chosen (as was done in deriving eq. (A4)) the Hankel function would have been of the second kind, $H_{n+\frac{1}{2}}^{(2)}(ka)$, as can be seen from 10.1.17, page 439 of [14] which yields e^{-iz} times a polynomial in $1/z$ for $h_n^{(1)}(z)$ and requires

$e^{+i\omega t}$ to generate a traveling wave. Note also that the sums in eqs. (A4) and (A20) are proportional since

$$2\int_{o}^{\pi} \frac{P_n^1(\cos\theta)}{\sin\theta}\, d\theta = 2\pi[P_n^1(\theta)]^2 \tag{A21}$$

which can be seen to be true by writing out the polynomial which represents $P_n^1(\cos\theta)$ and performing the operation indicated above term by term.

Now for a sphere that is small compared to a wavelength, the antenna input admittance in the transmitting case can be much less than the characteristic admittance of the guide which feeds the antenna. In this case the net voltage, V_o, into the load is

$$V_o = 2V_i \tag{A22a}$$

Therefore, the transmitting function of the sphere, $T_s(\omega,r,\frac{\pi}{2})$, which is given by eq. (A4) divided by V_i, can be expressed as a function of the receiving function of the sphere, $R_s(\omega)$, which is given by eq. (A20) divided by $G_L E_o$. In other words,

$$T_s(\omega,r,\tfrac{\pi}{2}) = \eta\omega\varepsilon\sqrt{\frac{2ka}{\pi}}\,\frac{e^{-ikr}}{kr}\sum_{n=1}^{\infty}\cdots \tag{A22b}$$

and

$$R_s(\omega) = \frac{i2\pi}{G_L\mu\omega}\sqrt{\frac{2ka}{\pi}}\sum_{n=1}^{\infty}\cdots \tag{A23}$$

Combining eqs. (A22) and (A23) yields

$$T_s(\omega,r,\tfrac{\pi}{2}) = \frac{i\eta G_L\omega^2\varepsilon\mu e^{-ikr}}{2\pi\ kr}\,R_s(\omega). \tag{A24}$$

This equation can be simplified using the identity,

$$\frac{\omega^2\mu\varepsilon}{2\pi k} = \frac{k}{2\pi} = \frac{1}{\lambda}\,. \tag{A25}$$

Therefore,

$$T_s(\omega,r,\tfrac{\pi}{2}) = i\eta G_L\,\frac{1}{\lambda r}\,e^{-ikr}\,R_s(\omega) \tag{A26}$$

is the required relation between the transmitting and receiving functions.

The broadband implication of eq. (A26) is that the ratio of T_s to R_s is inversely proportional to wavelength or, since

$$\frac{2\pi i}{\lambda} = \frac{i\omega}{c}\,, \tag{A27}$$

the impulse response in the time domain corresponding to T_s is the time derivative of the impulse response corresponding to R_s.

The above result has been derived for the specific case of a spherical antenna which could be solved in detail and for which we could see the effect of all the parameters. We will now show this result; namely that the transmitting transfer function is the time derivative of the receiving transfer function, is more general, and in fact can be obtained from general reciprocity relations.

Our equation for $T_h(\omega)$ can be written in a more general on axis form from eq. (1.61) of Kerns [16] as

$$T_h(\omega,r) = \frac{E_h(\omega,r)}{a_o(\omega)} \tag{A28}$$

$$= -ik\, \underline{S}_{10}(o)\, \frac{e^{ikr}}{r}$$

since

$$\gamma = k = \omega\sqrt{\mu\varepsilon} \quad \text{and} \quad \underline{R} = 0 \text{ on axis.}$$

The reception function into a matched load is found from eq. (1.6-9) of [16] to be

$$R_h(\omega) = \frac{b_o(\omega)}{E(\omega)}$$

$$= \frac{\underline{S}_{01}(o)\cdot\underline{A}}{E(\omega)} \tag{A29}$$

where $\underline{A}$ on axis is given by

$$\underline{A} = 2\pi\overline{E}(\omega)e^{-i\vec{k}\cdot\vec{r}}. \tag{A30}$$

Therefore

$$R_h(\omega) = S_{01}(o)2\pi e^{-ikr} \quad \text{on axis.} \tag{A31}$$

This can be recast in terms of $S_{10}(o)$ by the receprocity relation, eq. (1.6-20a), which is

$$\eta_o\underline{S}_{01}(o) = \sqrt{\frac{\varepsilon}{\mu}}\ \underline{S}_{10}(o) \tag{A32}$$

since $\gamma = k$. With eq. (A32) in eq. (A31) we obtain, at the reference plane,

$$R_h(\omega) = S_{10}(o)\,\frac{\sqrt{\frac{\varepsilon}{\mu}}}{\eta_o}\,2\pi. \tag{A33}$$

We can now obtain the generalized result for the ratio of $T_h(\omega)$ to $R_h(\omega)$ by dividing eq. (A28) by eq. (A33) which gives

$$\frac{T_h(\omega,r)}{R_h(\omega)} = \frac{-ikS_{10}(o)e^{ikr}/r}{S_{10}(o)\,\frac{\sqrt{\frac{\varepsilon}{\mu}}}{\eta_o}\,2\pi} \tag{A34}$$

$$= \frac{-i\eta_o}{\sqrt{\frac{\varepsilon}{\mu}}}\,\frac{1}{\lambda r}\,e^{ikr} \quad .$$

This result is identical with eq. (A26) for the sphere when one identifies the matched waveguide characteristic admittance, η_o in Kern's notation, with the load conductance, G_L, for the sphere and $1/\sqrt{\frac{\varepsilon}{\mu}}$ with the impedance, η, of free space.

This then yields the derivative relation between on axis, far-field radiated fields and plane wave receiving functions, but it is no longer restricted to a specific type of antenna. The waveguide used for all work reported was coaxial transmission line of Z_o impedance. When this is substituted into eq. (A34), the final form of the equation becomes,

$$\frac{T_h(\omega,r)}{R_h(\omega)} = \frac{-i\eta}{Z_o\lambda r}\,e^{ikr} \tag{A35}$$

APPENDIX B

Responses of Army Horn Antennas (Serial Nos. 7-76-1 and 7-76-3) in Both Receive and Transmit Modes With Appropriate Baluns

Freq. MHz	Receive Horn 1 dB	Receive Horn 3 dB	Transmit Horn 1 dB	Transmit Horn 3 dB
600	-34.2	-34.8	-10.4	-11.7
700	-35.2	-34.6	-10.5	- 9.8
800	-35.5	-35.5	-10.0	- 9.9
900	-35.2	-35.6	- 8.6	- 9.0
1000	-35.4	-35.0	- 8.1	- 7.4
1100	-34.9	-34.9	- 6.2	- 6.5
1200	-35.3	-35.4	- 5.8	- 5.7
1300	-35.3	-35.6	- 5.3	- 5.6
1400	-35.7	-35.6	- 4.7	- 4.7
1500	-35.7	-35.6	- 3.9	- 4.0
1600	-36.5	-37.6	- 4.2	- 5.8
1700	-36.9	-38.2	- 4.4	- 5.8
1800	-36.6	-37.5	- 3.7	- 4.3
1900	-37.1	-37.8	- 3.5	- 4.2
2000	-37.4	-37.7	- 3.6	- 3.6
2100	-36.6	-37.0	- 2.3	- 2.6
2200	-36.8	-37.3	- 1.8	- 2.6
2300	-37.3	-37.4	- 2.1	- 2.0
2400	-37.0	-37.3	- 1.1	- 1.3
2500	-37.1	-37.4	- 1.1	- 1.2
2600	-36.5	-37.3	- 0.4	- 1.2
2700	-36.6	-37.0	+ 0.1	- 0.1
2800	-37.0	-37.5	+ 0.3	+ 0.1
2900	-36.7	-37.8	+ 0.8	- 0.4
3000	-36.9	-36.9	+ 0.6	+ 0.8

Responses of Horns 1 and 3 Continued

Freq. MHz	Receive Horn 1 dB	Receive Horn 3 dB	Transmit Horn 1 dB	Transmit Horn 3 dB
3100	-36.9	-36.4	+ 1.1	+ 1.7
3200	-36.4	-37.1	+ 2.1	+ 1.4
3300	-36.5	-36.8	+ 2.0	+ 2.0
3400	-36.1	-35.6	+ 2.6	+ 3.1
3500	-35.9	-36.3	+ 3.2	+ 2.9
3600	-36.4	-36.7	+ 3.0	+ 2.7
3700	-36.5	-36.0	+ 3.0	+ 3.6
3800	-36.4	-36.6	+ 3.4	+ 3.4
3900	-36.4	-37.7	+ 4.0	+ 2.4
4000	-36.7	-37.4	+ 3.6	+ 2.9
4100	-37.6	-37.3	+ 2.9	+ 3.5
4200	-37.7	-38.3	+ 3.3	+ 2.8
4300	-38.1	-38.4	+ 2.4	+ 2.3
4400	-38.0	-37.3	+ 2.6	+ 3.4
4500	-37.7	-38.3	+ 4.2	+ 3.3
4600	-38.0	-39.0	+ 3.7	+ 2.8
4700	-38.4	-37.9	+ 3.0	+ 3.8
4800	-38.4	-38.4	+ 3.7	+ 3.8
4900	-39.0	-40.1	+ 3.7	+ 2.6
5000	-39.6	-40.0	+ 3.0	+ 2.6
5100	-40.5	-40.1	+ 2.1	+ 2.6
5200	-40.8	-42.1	+ 2.3	+ 0.9
5300	-41.3	-41.8	+ 1.6	+ 1.3
5400	-42.7	-41.3	+ 0.5	+ 2.0

REFERENCES

[1] Baum, C. E., Emerging technology for transient and broadband analysis and synthesis of antennas and scatterers, Proc. of IEEE, 64, No. 11, 1598-1616 (Nov. 1976).

[2] Susman, L., and Lamensdorf, D., Picosecond pulse antenna techniques, Rome Air Development Command Technical Report RADC-TR-71-64 (1971).

[3] Fitzgerald, D. J., and Martins, V. C., Impulse response measurement probes and instrumentation, Rome Air Development Command Technical Report, RADC-TR-74-288 (1974).

[4] Mayo, B. R., Howells, P. W., and Adams, W. B., Generalized linear radar analysis, Microwave Journal, 4, 79 (1961).

[5] Martins, V. C., and Van Meter, J. L., Picosecond pulse reflector antenna investigation, Rome Air Development Command Technical Report, RADC-TR-73-215 (1973).

[6] Ramo, S., Whinnery, J. R., and VanDuzer, T., Fields and waves in communication electronics, (J. Wiley and Sons Inc., New York , N.Y., 1965).

[7] Gans, W. L., and Andrews, J. R., Time domain automatic network analyzer for measurement of rf and microwave components, National Bureau of Standards Technical Note 672 (Sept. 1975).

[8] Gans, W. L., Present capabilities of the NBS automatic pulse measurement system, IEEE Trans. on Instr. and Meas., IM-25, No. 4, 384-388 (Dec. 1976).

[9] Andrews, J. R. and Gans, W. L., Time domain automatic network analyzer, L'onde électrique, 55, No. 10, 569-574 (Oct. 1975).

[10] Riad, S. M., The theory and application of the homomorphic transformation to time domain spectroscopy and scattering problems, Ph.D. Dissertation, Univ. of Toledo (Aug. 1976).

[11] Kanda, M., A Relatively Short Cylindrical Broadband Antenna With Tapered Resistive Loading for Picosecond Pulse Measurements, IEEE Trans. Ant. & Prop., Vol. AP-26, No. 3, 439-447 (May 1978).

[12] Andrews, J. R., Proceedings of the 1975 IEEE Symposium on EMC (Oct. 1975).

[13] Andrews, J. R., and Arthur, M. G. Spectrum amplitude, definition, generation and measurement, NBS Technical Note 699 (Oct. 1977).

[14] Abramowitz, M., and Stegun, I. A., Handbook of mathematical functions (Dover Publications Inc., New York, N.Y., 1965).

[15] Stratton, J. A., Electromagnetic theory (McGraw-Hill, New York, N.Y. 1941).

[16] Kerns, D. M., Plane-wave scattering theory of antennas and antenna-interactions: formulation and applications, J. Res. Nat. Bur. Stand. (U.S.), 80B (Math. Sci.), No. 1, (Jan-Mar. 1976).

NBS-114A (REV. 7-73)

U.S. DEPT. OF COMM. BIBLIOGRAPHIC DATA SHEET	1. PUBLICATION OR REPORT NO. NBS TN-1008	2. Gov't Accession No.	3. Recipient's Accession No.

4. TITLE AND SUBTITLE

Antennas and the Associated Time Domain Range for the Measurement of Impulsive Fields

5. Publication Date

November 1978

6. Performing Organization Code

724.04

7. AUTHOR(S)

R. A. Lawton and Arthur R. Ondrejka

8. Performing Organ. Report No.

9. PERFORMING ORGANIZATION NAME AND ADDRESS

NATIONAL BUREAU OF STANDARDS
DEPARTMENT OF COMMERCE
WASHINGTON, D.C. 20234

10. Project/Task/Work Unit No.

7244153

11. Contract/Grant No.

12. Sponsoring Organization Name and Complete Address *(Street, City, State, ZIP)*

Same as Item 9.

13. Type of Report & Period Covered

14. Sponsoring Agency Code

15. SUPPLEMENTARY NOTES

16. ABSTRACT *(A 200-word or less factual summary of most significant information. If document includes a significant bibliography or literature survey, mention it here.)*

This report describes the construction and evaluation of a TEM horn antenna designed at NBS to be used as a transfer standard to generate and measure impulsive electromagnetic fields. Our purpose in the evaluation was to analyze the different electrical field generation and measurement techniques thoroughly enough to determine the major sources of error and establish a standard of impulsive field strength having a well established statement of accuracy.

The evaluation of this horn was done in two independent ways; by placing the horn in the field of a conical transmission line and by a three antenna intercomparison. The two methods were found to agree within ± 3 dB over the range of 0.6 to 5 GHz. Part of this disagreement is due to the assumption of far field conditions, and an experimental technique is described which determines the frequency range over which this assumption is valid.

17. KEY WORDS *(six to twelve entries; alphabetical order; capitalize only the first letter of the first key word unless a proper name; separated by semicolons)*

Antenna; conical transmission line; impulsive fields; impulse response; standards; TEM horn antenna.

18. AVAILABILITY [XX] Unlimited

[ ] For Official Distribution. Do Not Release to NTIS

[X] Order From Sup. of Doc., U.S. Government Printing Office Washington, D.C. 20402, XXXXXXXXXXX

[ ] Order From National Technical Information Service (NTIS) Springfield, Virginia 22151

19. SECURITY CLASS (THIS REPORT)	21. NO. OF PAGES
UNCLASSIFIED	68
20. SECURITY CLASS (THIS PAGE)	**22. Price**
UNCLASSIFIED	$2.40

☆U.S. GOVERNMENT PRINTING OFFICE: 1978-0-677-072/1209 USCOMM-DC 29042-P74

NBS TECHNICAL PUBLICATIONS

PERIODICALS

JOURNAL OF RESEARCH—The Journal of Research of the National Bureau of Standards reports NBS research and development in those disciplines of the physical and engineering sciences in which the Bureau is active. These include physics, chemistry, engineering, mathematics, and computer sciences. Papers cover a broad range of subjects, with major emphasis on measurement methodology, and the basic technology underlying standardization. Also included from time to time are survey articles on topics closely related to the Bureau's technical and scientific programs. As a special service to subscribers each issue contains complete citations to all recent NBS publications in NBS and non-NBS media. Issued six times a year. Annual subscription: domestic $17.00; foreign $21.25. Single copy, $3.00 domestic; $3.75 foreign.

Note: The Journal was formerly published in two sections: Section A "Physics and Chemistry" and Section B "Mathematical Sciences."

DIMENSIONS/NBS

This monthly magazine is published to inform scientists, engineers, businessmen, industry, teachers, students, and consumers of the latest advances in science and technology, with primary emphasis on the work at NBS. The magazine highlights and reviews such issues as energy research, fire protection, building technology, metric conversion, pollution abatement, health and safety, and consumer product performance. In addition, it reports the results of Bureau programs in measurement standards and techniques, properties of matter and materials, engineering standards and services, instrumentation, and automatic data processing.

Annual subscription: Domestic, $11.00; Foreign $13.75

NONPERIODICALS

Monographs—Major contributions to the technical literature on various subjects related to the Bureau's scientific and technical activities.

Handbooks—Recommended codes of engineering and industrial practice (including safety codes) developed in cooperation with interested industries, professional organizations, and regulatory bodies.

Special Publications—Include proceedings of conferences sponsored by NBS, NBS annual reports, and other special publications appropriate to this grouping such as wall charts, pocket cards, and bibliographies.

Applied Mathematics Series—Mathematical tables, manuals, and studies of special interest to physicists, engineers, chemists, biologists, mathematicians, computer programmers, and others engaged in scientific and technical work.

National Standard Reference Data Series—Provides quantitative data on the physical and chemical properties of materials, compiled from the world's literature and critically evaluated. Developed under a world-wide program coordinated by NBS. Program under authority of National Standard Data Act (Public Law 90-396).

NOTE: At present the principal publication outlet for these data is the Journal of Physical and Chemical Reference Data (JPCRD) published quarterly for NBS by the American Chemical Society (ACS) and the American Institute of Physics (AIP). Subscriptions, reprints, and supplements available from ACS, 1155 Sixteenth St. N.W., Wash., D.C. 20056.

Building Science Series—Disseminates technical information developed at the Bureau on building materials, components, systems, and whole structures. The series presents research results, test methods, and performance criteria related to the structural and environmental functions and the durability and safety characteristics of building elements and systems.

Technical Notes—Studies or reports which are complete in themselves but restrictive in their treatment of a subject. Analogous to monographs but not so comprehensive in scope or definitive in treatment of the subject area. Often serve as a vehicle for final reports of work performed at NBS under the sponsorship of other government agencies.

Voluntary Product Standards—Developed under procedures published by the Department of Commerce in Part 10, Title 15, of the Code of Federal Regulations. The purpose of the standards is to establish nationally recognized requirements for products, and to provide all concerned interests with a basis for common understanding of the characteristics of the products. NBS administers this program as a supplement to the activities of the private sector standardizing organizations.

Consumer Information Series—Practical information, based on NBS research and experience, covering areas of interest to the consumer. Easily understandable language and illustrations provide useful background knowledge for shopping in today's technological marketplace.

Order **above** *NBS publications from: Superintendent of Documents, Government Printing Office, Washington, D.C. 20402.*

Order **following** *NBS publications—NBSIR's and FIPS from the National Technical Information Services, Springfield, Va. 22161.*

Federal Information Processing Standards Publications (FIPS PUB)—Publications in this series collectively constitute the Federal Information Processing Standards Register. Register serves as the official source of information in the Federal Government regarding standards issued by NBS pursuant to the Federal Property and Administrative Services Act of 1949 as amended, Public Law 89-306 (79 Stat. 1127), and as implemented by Executive Order 11717 (38 FR 12315, dated May 11, 1973) and Part 6 of Title 15 CFR (Code of Federal Regulations).

NBS Interagency Reports (NBSIR)—A special series of interim or final reports on work performed by NBS for outside sponsors (both government and non-government). In general, initial distribution is handled by the sponsor; public distribution is by the National Technical Information Services (Springfield, Va. 22161) in paper copy or microfiche form.

BIBLIOGRAPHIC SUBSCRIPTION SERVICES

The following current-awareness and literature-survey bibliographies are issued periodically by the Bureau:

Cryogenic Data Center Current Awareness Service. A literature survey issued biweekly. Annual subscription: Domestic, $25.00; Foreign, $30.00.

Liquified Natural Gas. A literature survey issued quarterly. Annual subscription: $20.00.

Superconducting Devices and Materials. A literature survey issued quarterly. Annual subscription: $30.00. Send subscription orders and remittances for the preceding bibliographic services to National Bureau of Standards, Cryogenic Data Center (275.02) Boulder, Colorado 80302.

U.S. DEPARTMENT OF COMMERCE
National Bureau of Standards
Washington, D.C. 20234

OFFICIAL BUSINESS

Penalty for Private Use, $300

POSTAGE AND FEES PAID
U.S. DEPARTMENT OF COMMERCE
COM-215

U.S.MAIL

SPECIAL FOURTH-CLASS RATE
BOOK